European Journal of Medicinal Chemistry 183 (2019) 111716

Contents lists available at ScienceDirect

European Journal of Medicinal Chemistry

journal homepage: http://www.elsevier.com/locate/ejmech

Research paper

Design, synthesis and biological evaluation of novel 7*H*-pyrrolo[2,3-*d*] pyrimidine derivatives as potential FAK inhibitors and anticancer agents

Ruifeng Wang [a], Yixuan Chen [a, b], Xiangxin Zhao [a], Sijia Yu [a], Bowen Yang [a], Tianxiao Wu [a], Jing Guo [a], Chenzhou Hao [a], Dongmei Zhao [a, *], Maosheng Cheng [a]

[a] Key Laboratory of Structure-Based Drug Design and Discovery, Ministry of Education, School of Pharmaceutical Engineering, Shenyang Pharmaceutical University, 103 Wenhua Road, Shenhe District, Shenyang, 110016, China
[b] The School of Life Science and Biopharmaceutical, Shenyang Pharmaceutical University, 103 Wenhua Road, Shenhe District, Shenyang, 110016, China

ARTICLE INFO

Article history:
Received 11 August 2019
Received in revised form
17 September 2019
Accepted 17 September 2019
Available online xxx

Keywords:
FAK inhibitor
Structure-activity relationship
7*H*-pyrrolo[2,3-*d*]pyrimidine
Dimethylphosphine oxide
Anticancer
Molecular docking

ABSTRACT

A series of 7*H*-pyrrolo[2,3-*d*]pyrimidine derivatives possessing a dimethylphosphine oxide moiety were designed, synthesized and evaluated as novel Focal adhesion kinase (FAK) inhibitors. Most compounds potently suppressed the enzymatic activities of FAK, with IC_{50} values in the 10^{-8}–10^{-9} M range, and potently inhibited the proliferation of breast (MDA-MB-231) and lung (A549) cancer cell lines. The representative compound **25b** exhibited potent enzyme inhibition ($IC_{50} = 5.4$ nM) and good selectivity when tested on a panel of 26 kinases. **25b** exhibited antiproliferative activity against A549 cells ($IC_{50} = 3.2\ \mu M$) and relatively less cytotoxicity to a normal human cell line HK2. Compound **25b** also induced apoptosis and suppressed the migration of A549 cells in a concentration-dependent manner. Further profiling of compound **25b** revealed it had good metabolic stability in mouse, rat and human liver microsomes *in vitro* and showed weak inhibitory activity against various subtypes of human cytochrome P450. The docking study of compound **25b** was performed to elucidate its possible binding modes and to provide a structural basis for further structure-guided design of FAK inhibitors.

1. Introduction

Focal adhesion kinase (FAK) is a cytoplasmic tyrosine kinase that has been identified as a key regulator of growth factor receptor- and integrin-mediated signals. FAK governs fundamental processes in cancer and normal cells through its kinase activity and scaffolding function [1–3]. FAK overexpression has been documented in multiple tumor types, including prostate, breast, lung, ovarian, neck, head and colon cancer, and it has been correlated with poor prognosis of cancer patients [3,4]. FAK promotes malignancy by regulating tumorigenic and metastatic potential through highly coordinated signaling networks that orchestrate a diverse range of cellular processes, such as cell proliferation, survival, invasion, migration, angiogenesis, epithelial–mesenchymal transition and regulation of cancer stem cell activities [5–8]. Similarly, studies using dominant negative FAK mutants, antisense oligonucleotides and siRNA to FAK have exemplified the role of FAK in cancer cell progression and metastasis [9,10]. More importantly, recent research has identified FAK as a key mediator of the immune response in certain cancers and has shown that targeting FAK renders pancreatic cancers responsive to checkpoint immunotherapy [11,12]. Furthermore, FAK is a novel regulator of DNA damage repair in mutant KRAS NSCLC, and its pharmacologic inhibition leads to radiosensitizing effects that could be beneficial in cancer therapy [13]. Thus, the FAK enzyme has emerged as a promising cancer therapeutic target.

Several potent and selective FAK inhibitors have been designed and developed, and some compounds have entered preclinical or clinical trials (see Fig. 1), including TAE226 (1) [14], VS-4718 (2, phase I, NCT01849744) [15], CEP-37440 (3, phase I, NCT01922752) [16], defactinib (4, phase II, NCT02465060) [17], PF-562271 (5, phase I, NCT00666926) [18], and GSK2256098 (6, phase II, NCT02428270, NCT02523014) [19]. These compounds are orally bioavailable, ATP competitive inhibitors of FAK, and they exhibit highly potent inhibitory activity toward FAK and potent antitumor

* Corresponding author.
E-mail address: Medchemzho@163.com (D. Zhao).

https://doi.org/10.1016/j.ejmech.2019.111716
0223-5234/

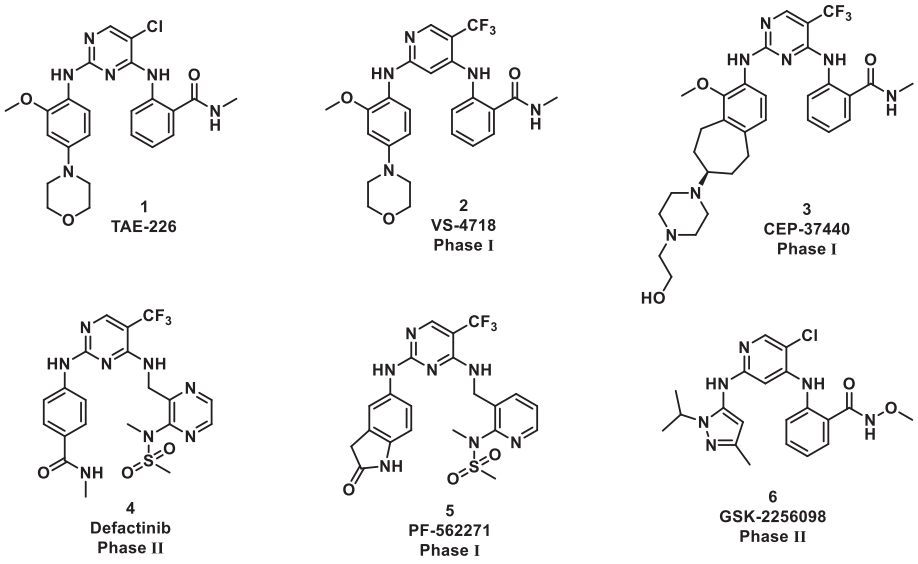

Fig. 1. Structures of potent and selective FAK inhibitors.

activities in a panel of *in vitro* and in vivo cancer models. Moreover, the progress in evaluating FAK inhibitors in both preclinical models and human clinical trials is promising. Therefore, the aim of the work reported herein was to identify a novel scaffold from which to develop new FAK inhibitors as anticancer agents.

It was observed that 2,4-diaminopyridine and 2,4-diaminopyrimidine are the major scaffolds found in compounds described by pharmaceutical companies and academic research [20–22]. In this study, we presented additional medicinal chemistry efforts performed on this scaffold, focusing on the replacement of the 2,4-diaminopyridine scaffold by the 7*H*-pyrrolo[2,3-*d*] pyrimidine-2,4-diamine scaffold. We assumed it was feasible to introduce an extra interaction with Glu500 by a simple addition of a hydrogen donor in this region, which would result in hinge-binding moiety containing three donor–acceptor interactions instead of two in the pyrimidine case. In addition, various substituents with hydrogen bond receptors were introduced at R_1 to form hydrogen bond interactions with Asp564 of the DFG motif. Compounds containing a dimethylphosphine oxide (DMPO) moiety exhibited better activity to FAK. Given this result, we retained the ortho-DMPO-substituted benzene at R_1 to further explore SAR at R_2. Further modifications were performed by introducing a substituted benzene ring or substituted pyrazole ring at the R_2 to improve potency and adjust drug-like properties (see in Fig. 2). On the basis of the above strategies, this paper describes the design, synthesis, biological evaluation, and docking study of 7*H*-pyrrolo[2,3-*d*]pyrimidine derivatives as novel FAK inhibitors.

2. Chemistry

Compounds **11a-h** as well as intermediates **14** and **17** were synthesized as depicted in Scheme 1. Commercially available 2,4-dichloro-7*H*-pyrrolo[2,3-*d*]pyrimidine (**7**) was protected by TsCl to afford intermediate **8**, which was equipped with a variety of substituted anilines or benzylamines via S_NAr reactions under basic conditions to afford intermediates **9a-d**. Palladium-catalyzed Buchwald cross-coupling with corresponding substituted anilines afforded intermediates **10a-h** [23], and was followed by a deprotection step to remove the Ts-protection group to produce target compounds **11a-h**. S_NAr reactions between 2-fluorobenzonitrile (**12**) and *N*-methylmethane-sulfonamide were conducted under basic conditions to afford intermediate **13**, which was then subjected to reduction by BH_3 in THF to yield intermediate **14**. *N*-methylation of 3-nitropyridin-2(1*H*)-one (**15**) followed by

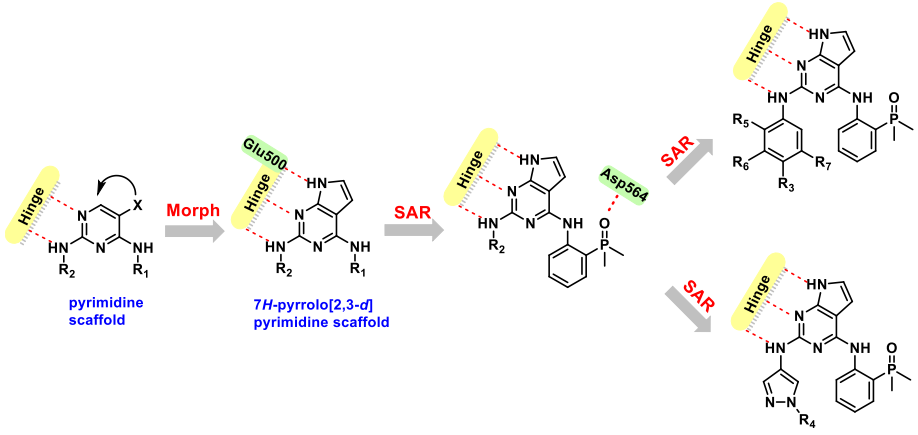

Fig. 2. Rational design of target compounds.

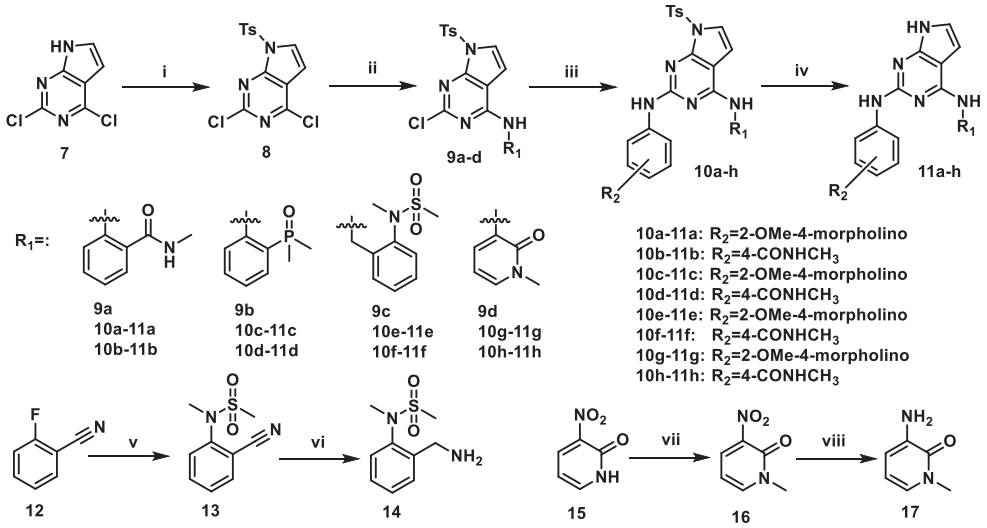

Scheme 1. Synthesis of compounds **11a-h** and intermediates **14** and **17**. Reagents and conditions: (i) Ts-Cl, NaH, anhydrous THF, 0 °C; (ii) NH_2-R_1, DIPEA, n-BuOH, 100 °C; (iii) 4-amino-*N*-methylbenzamide or 2-methoxy-4-morpholinoaniline, $Pd(AcO)_2$, X-phos, Cs_2CO_3, dioxane, 90 °C; (iv) NaOH, MeOH/H_2O, 40 °C. (v) *N*-methylmethanesulfonamide, Cs_2CO_3, CH_3CN, 80 °C; (vi) BH_3 (2M in THF), anhydrous THF, 60 °C; (vii) iodomethane, NaH, anhydrous THF, 55 °C; (viii) Pd/C, H_2, MeOH, 40 °C.

reduction of nitro (H_2, Pd/C) generated intermediate **17**. Compounds **20a-l**, **22a-g** and **25a-h** were prepared under reaction conditions similar to those depicted in Scheme 2. The synthesis of compounds **25a-h** is used as an example for illustration. Buchwald cross-coupling of **9b** with appropriate substituted amines in the presence of $Pd(AcO)_2$, X-phos and Cs_2CO_3 or $Pd(dba)_2$, BINAP and Cs_2CO_3 gave the intermediates **23a-h**. Then, the tosyl group was subsequently removed under basic conditions (NaOH, MeOH/H_2O) to give intermediates **24a-h**. An additional deprotection step removing the Boc-protection group of the solubilizing tail was conducted to produce target compounds **25a-h**. Intermediates **28a-f** and **31a-h** were synthesized as depicted in Scheme 3. The starting 1*H*-pyrazol-4-amine (**26**) underwent a Mitsunobu reaction with corresponding alcohols to afford intermediates **27a-c** [24], and it underwent an electrophilic substitution reaction with corresponding halogenated substance to afford intermediates **27d-f**. The nitro group was then reduced by Pd/C in the presence of H_2 to yield amines **28a-f**. Coupling of acids **29a-h** with tert-butyl 4-aminopiperidine-1-carboxylate in the presence of HATU and DIPEA followed by nitro-reduction provided intermediates **31a-h** [25]. Compounds **34b**, **35**, **38b** and **39** were synthesized as depicted in Scheme 4. We performed the three-step reaction sequence mentioned above, consisting of S_NAr reaction, Buchwald cross-coupling and deprotection, to synthesize these compounds.

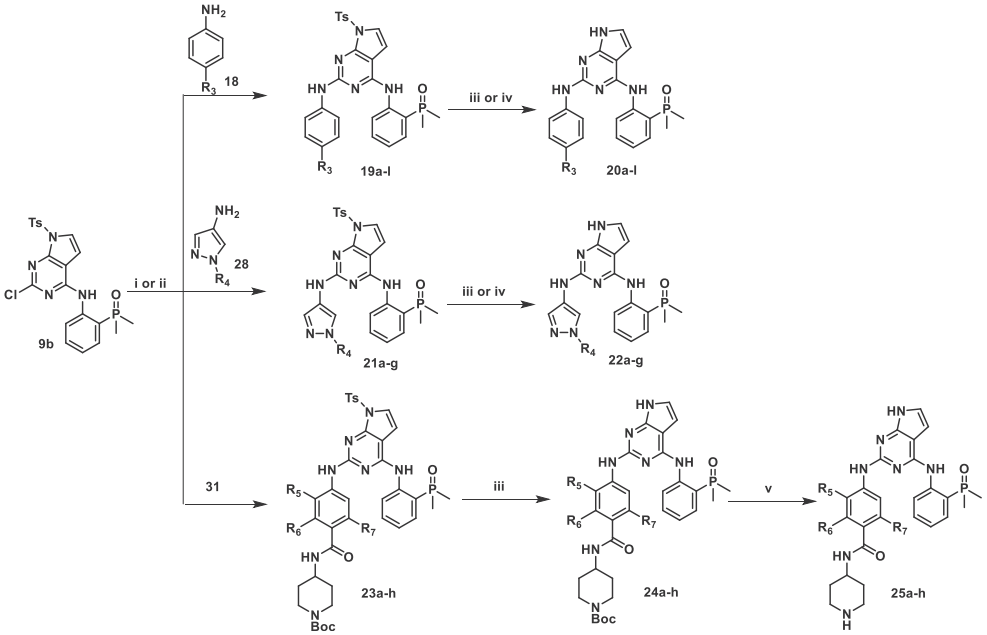

Scheme 2. Synthesis of compounds **20a-l**, **22a-g** and **25a-h**. Reagents and conditions: (i) corresponding aromatic amines, $Pd(AcO)_2$, X-phos, Cs_2CO_3, dioxane, 90 °C; (ii) corresponding aromatic amines, $Pd(dba)_2$, BINAP, Cs_2CO_3, dioxane, 90 °C; (iii) NaOH, MeOH/H_2O, 40 °C; (iv) a) NaOH, MeOH/H_2O, 40 °C; b) HCl-EA, rt; (v) HCl-EA, rt.

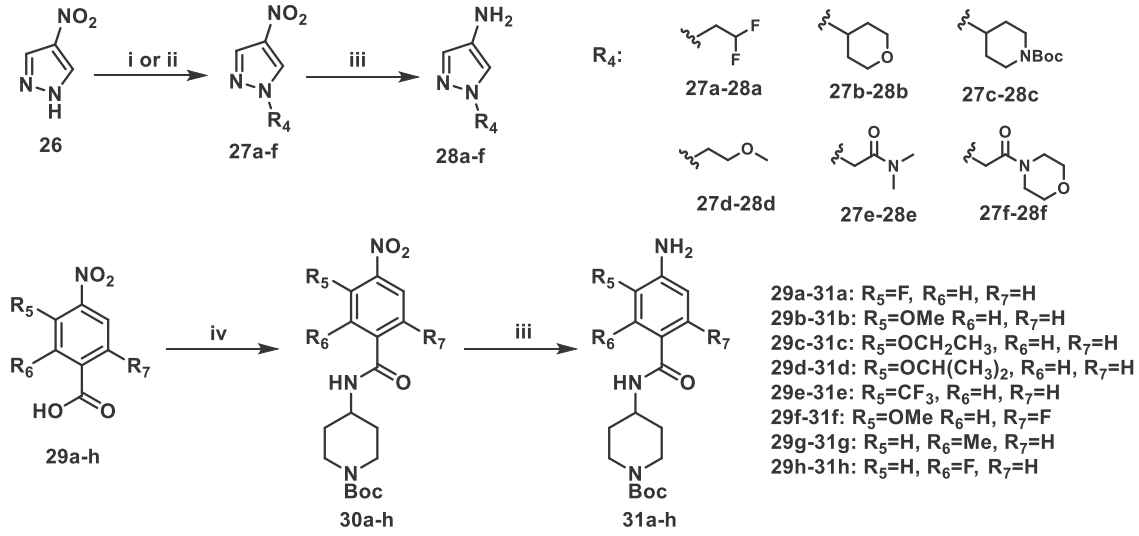

Scheme 3. Synthesis of intermediates **28a-f** and **31a-h**. Reagents and conditions: (i) for **27a-c**, R_4-OH, PPh_3, DEAD, THF, rt; (ii) for **27d-f**, R_4-Br, K_2CO_3, DMF, 40 °C-80 °C; (iii) Pd/C, H_2, EtOH, 40 °C; (iv) tert-butyl 4-aminopiperidine-1-carboxylate, HATU, DIPEA, CH_2Cl_2, 25 °C-40 °C.

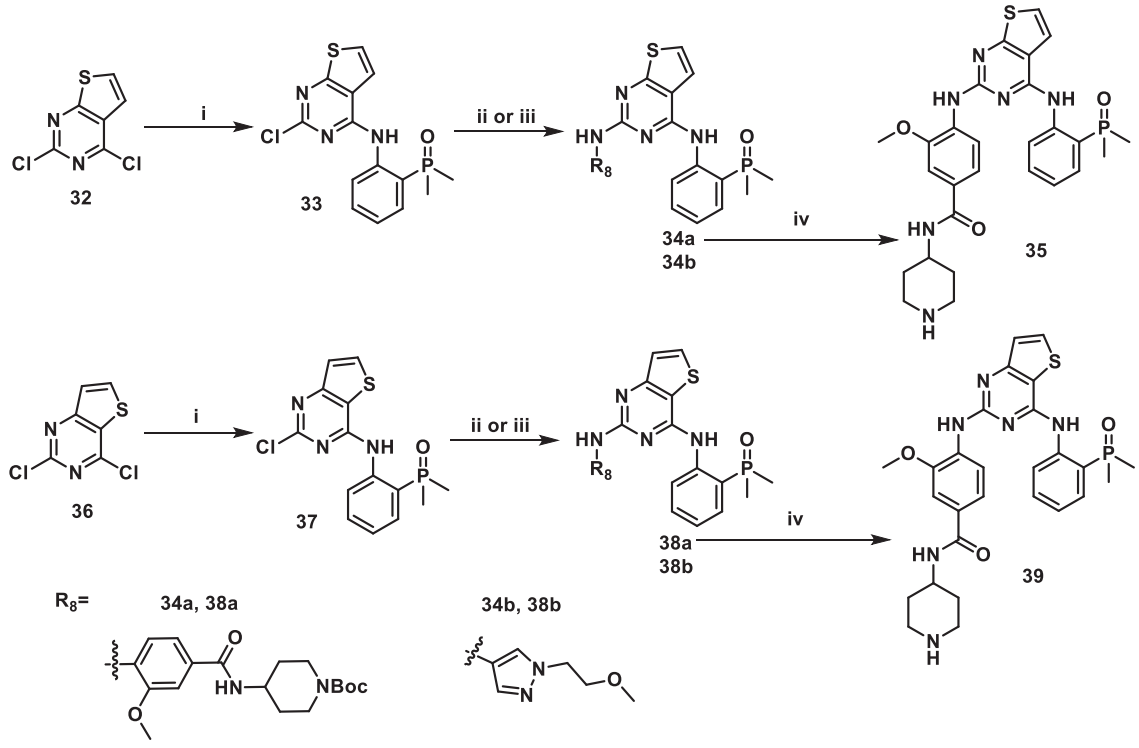

Scheme 4. Synthesis of compounds **34b**, **38b**, **35** and **39**. Reagents and conditions: (i) (2-aminophenyl) dimethylphosphine oxide, DIPEA, DMF, 110 °C; (ii) R_8-NH_2, $Pd(AcO)_2$, X-phos, Cs_2CO_3, dioxane, 90 °C; (iii) R_8-NH_2, $Pd(dba)_2$, BINAP, Cs_2CO_3, dioxane, 90 °C; (iv) HCl-EA, rt.

3. Results and discussion

3.1. In vitro activity against FAK kinase and SAR analyses

All newly synthesized compounds were evaluated for their activity against the FAK enzyme using homogeneous time-resolved fluorescence (HTRF) assays, and TAE-226 was tested for comparison. Under the experimental conditions, TAE-226 displayed strong inhibition against FAK with an IC_{50} value of 6.2 nM, which was similar to the previously reported data [21].

As the starting point, we introduced the dominant fragments of the reported inhibitors at the R_2 moiety (Table 1). Introduction of the *N*-methyl-2-benzamide moiety at R_1 led to compounds **11a** and **11b**, which retained moderate potency against FAK (IC_{50} values of 34.5 and 91.8 nM, respectively), indicating that the 7*H*-pyrrolo[2,3-*d*]pyrimidine scaffold was suitable for developing new FAK inhibitors. The different fragments with hydrogen bond receptors at R_1 were introduced to form hydrogen bond interaction with Asp564 of the DFG motif. The results indicated that the dimethyl(phenyl)phosphine oxide or *N*-methyl-*N*-phenylmethanesulfonamide moiety at

Table 1
The FAK enzymatic activities of compounds **11a-h**.

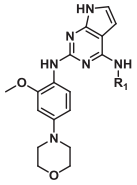
11a, 11c, 11e, 11g

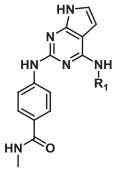
11b, 11d, 11f, 11h

Compd.	R_1	IC_{50} (nM)[a]	Compd.	R_1	IC_{50} (nM)[a]
11a	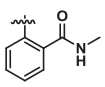	34.5	**11e**	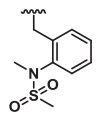	31.9
11b		91.8	**11f**		17.1
11c		51.1	**11g**		150.8
11d		15.5	**11h**		126.4
TAE-226		6.2			

[a] The IC_{50} values are shown as the mean (nM) values from two separate experiments.

R_1 (**11c-f**) retained potent activity against FAK with IC_{50} values between 15.5 and 51.1 nM. Replacement of the R_1 group by a pyridone-containing fragment (**11g**, **11h**) resulted in decreased activity toward FAK ($IC_{50} > 100$ nM). In particular, compound **11d**, which contained a DMPO moiety, exhibited better activity to FAK ($IC_{50} = 15.5$ nM). Although phosphorus is abundant in the human body, it is rarely found in drug molecules, and phosphine oxide is an overlooked but novel hydrogen bond acceptor [26]. To further explore the potential of this functionality, we incorporated DMPO into the design of FAK inhibitors.

On the basis of compound **11d**, we next focused SAR exploration on the R_3 position. As shown in Table 2, the introduction of amide, sulfonamide or phosphate-containing fragments as R_3 yielded compounds **20a-c**, which exhibited lower potency against FAK with IC_{50} values between 38.7 and 85.0 nM. Due to the para-substitution vector R_3 pointing toward the solvent region, the introduction of a hydrophilic fragment at the R_3 position may contribute to activity enhancement. A class of diverse hydrophilic fragment-containing derivatives (**20d-l**) were designed and synthesized, and most compounds exhibited potent inhibitory activity against FAK. Among these derivatives, addition of the piperidineyl group to compound **11d** gave compound **20d,** which significantly increased the activity toward FAK ($IC_{50} = 6.8$ nM). Substitution of the terminal piperidineyl in **20d** by tetrahydro-pyranyl (**20e**) or 1-methylpiperidineyl (**20f**) led to reduced FAK potency. The R-enantiomer **20g** exhibited lower potency against FAK ($IC_{50} = 64.4$ nM), but was less potent compared to the S-enantiomer **20h** ($IC_{50} = 9.1$ nM). Morpholine or piperazine ring attached to the C_2 phenyl via a carbonyl group yielded compounds **20i-j**, which were less potent than compounds **20d-e**. The compound bearing a *N*-methylpiperazine (**20k**) directly attached to C_2 phenyl displayed moderate potency ($IC_{50} = 21.9$ nM), and 2-fold higher potency ($IC_{50} = 9.3$ nM) was observed for a piperazine-substituted analogue **20l**.

Compounds **22a-g** represent a series of analogs bearing a (1-substituted)-1*H*-pyrazo-4-yl moiety. As shown in Table 3, the methyl-substituted compound **22a** and 1,1-difluoroethyl-substituted analog **22b** were equally potent (156.1 vs 132.6 nM), but much higher potency ($IC_{50} = 23.1$ nM) was observed for the methoxyethyl-substituted pyrazole **22c**. The tetrahydro-pyran-4-yl-substituted pyrazole **22d** exhibited moderate potency against FAK ($IC_{50} = 64.1$ nM), and much higher potency ($IC_{50} = 26.2$ nM) was observed for the piperidin-4-yl-substituted analog **22e**. Compound **21f** bearing a flexible acetamide moiety showed poor potency ($IC_{50} = 176.2$ nM), but much higher potency ($IC_{50} = 21.1$ nM) was observed for the morpholine-substituted analog **22g**.

Table 2
The FAK enzymatic activities of compounds **20a-l**.

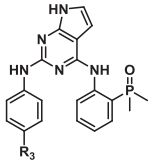

Compd.	R_3	IC_{50} (nM)[a]	Compd.	R_3	IC_{50} (nM)[a]
11d		15.8	**20g**		64.4
20a		85.0	**20h**		9.1
20b		38.7	**20i**		38.2
20c		82.0	**20j**		62.1
20d	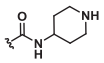	6.8	**20k**		21.9
20e		16.7	**20l**		9.3
20f	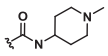	17.2	**TAE-226**		6.2

[a] The IC_{50} values are shown as the mean (nM) values from two separate experiments.

Table 3
The FAK enzymatic activities of compounds 22a-g.

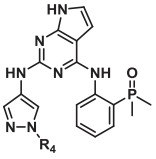

Compd.	R_4	IC_{50} (nM)[a]	Compd.	R_4	IC_{50} (nM)[a]
22a	CH_3	156.1	**22e**		26.2
22b		132.6	**22f**		176.6
22c	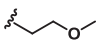	23.1	**22g**	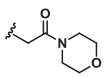	21.1
22d		64.1	**TAE-226**		6.2

[a] The IC_{50} values are shown as the mean (nM) values from two separate experiments.

Because compound **20d** exhibited the best activity and moderate stability in mouse liver microsomes ($T_{1/2} = 92.9$ min), we studied its binding modes with FAK by molecular docking to guide the next round of structural optimization. As shown in Fig. 3A, compound **20d** binds to FAK in the ATP-binding site by adopting a U-shaped ligand conformation. Briefly, the main interactions include molecular interactions of the 7*H*-pyrrol[2,3-*d*]pyrimidine scaffold with the hinge region, molecular interactions of the DMPO moiety with the Asp564 of the DFG motif, and molecular interactions of the piperidine moiety with Cys427. As shown in Fig. 3B, it's worth noting that the gatekeeper+2 residue is a smaller Leu501 for FAK, but it is a bulky Phe or Tyr for most kinases [27]. Therefore, the substituents on the 2-*N*-aryl will occupy the lower hinge area pocket and hydrophobically interact with the side chain of Leu501, which can potentially improve the selectivity of the kinase family.

Based on the above analysis, we started the optimization study of compound **20d** by varying the substituent on the benzene ring. As shown in Table 4, introducing F-, MeO- or EtO- as the R_5 or Me- or F- as the R_6 yielded compounds **25a-c** and **25g-h**, which retained high potency against FAK, with IC_{50} values between 5.1 and 14.0 nM. Similarly, fluoro group introduction para to the methoxy substituent on the 2-substituted aniline resulted in a potent inhibitor **25f** ($IC_{50} = 9.4$ nM). Further substituting the R_6 moiety to larger i-PrO (**25d**) and CF_3 (**25e**) groups resulted in remarkable activity loss toward FAK ($IC_{50} = 80.8$ nM and 347.5 nM, respectively).

Finally, on the basis of representative compounds **22c** and **25b**, bioisostere substitution was performed on the 7*H*-pyrrolo[2,3-*d*]pyrimidine scaffold to obtain compounds **34b**, **35**, **38b** and **39** (Table 5). Compared to compound **22c**, the thieno[2,3-*d*]pyrimidine analogs **34b** and **38b** were more than 5-fold less potent against FAK. Similarly, lower potency was observed for the thieno[2,3-*d*]pyrimidine analogs **35** and **39** compared to compound **25b**. These results indicated that hydrogen bonding of the 7*H*-pyrrolo[2,3-*d*]pyrimidine and Glu500 contributes to achieving high potency.

3.2. Kinase selectivity profile

To obtain detailed information for the selectivity profile of this series, the potent inhibitor **25b** was further subjected to kinase selectivity profiling with a panel of 26 kinases at a concentration of 0.5 μM, and the percent inhibition values were reported in Table 6. Good kinase selectivity was observed for **25b**, with only FAK and ALK producing greater than 80% inhibition. Three kinases (SYK, PLK1 and TBK1) were inhibited by **25b** to an extent of 20%–80%. For the other 21 kinases, the inhibition rate was less than 20%.

Table 4
The FAK enzymatic activities of compounds **25a-h**.

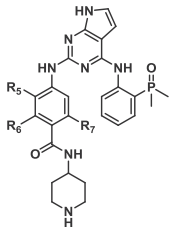

Compd.	R_5	R_6	R_7	IC_{50} (nM)[a]
20d	H	H	H	6.8
25a	F	H	H	14.0
25b	OMe	H	H	5.4
25c	OCH_2CH_3	H	H	5.8
25d	$OCH(CH_3)_2$	H	H	80.8
25e	CF_3	H	H	347.5
25f	OMe	H	F	9.4
25g	H	Me	H	10.3
25h	H	F	H	5.1
TAE-226				6.2

[a] The IC_{50} values are shown as the mean (nM) values from two separate experiments.

Table 5
The FAK enzymatic activities of compounds **34b, 35, 38b** and **39**.

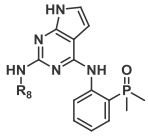
22c, 25b

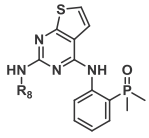
34b, 35

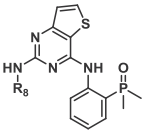
38b, 39

Compd.	R_8	IC_{50} (nM)[a]	Compd.	R_8	IC_{50} (nM)[a]
22c	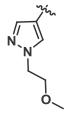	23.1	**25b**	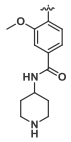	5.4
34b		185.6	**35**		23.0
38b		154.2	**39**		20.6
TAE-226		6.2			

[a] The IC_{50} values are shown as the mean (nM) values from two separate experiments.

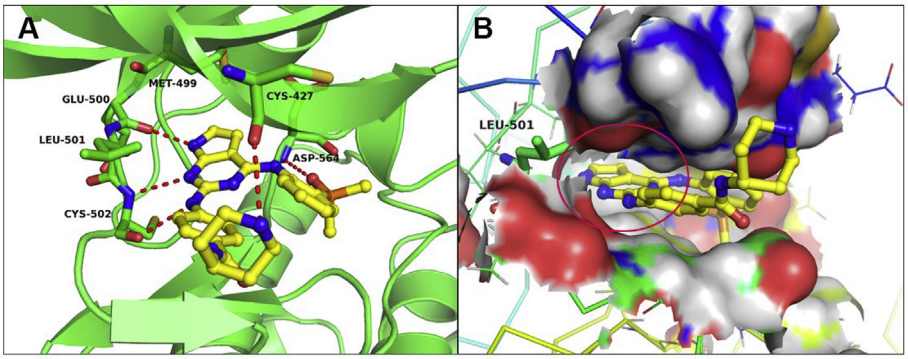

Fig. 3. Molecular docking model of compound **20d** in the FAK active site. (A) Detailed interactions with the protein residues. Each dashed red line represents a hydrogen bond. (B) The red frame represents the lower hinge area pocket. (For interpretation of the references to colour in this figure legend, the reader is referred to the Web version of this article.)

Table 6
Kinase selectivity profile of compound **25b**.[a]

Kinase	%inhibition at 0.5 μM	kinase	%inhibition at 0.5 μM	kinase	%inhibition at 0.5 μM
ABL1	5	HER2	12	PIM2	−3
AKT1	0	FGFR1	6	PLK1	43
ALK	98	FLT3	13	PKA	2
BRAF	3	mTOR	0	FAK	100
BTK	0	KDR	1	SYK	73
CDK2	1	KIT	2	RET	10
CHK1	3	LCK	14	TBK1	23
CSF1R	12	ERK2	9	ZAP70	−3
DDR2	1	cMet	−2		

Profiling Service from Life Technologies. The results represent the mean of three independent experiments performed in triplicate.
[a] Selectivity profile of compound **25b** measured at a concentration of 0.5 μM in a panel of 26 kinases generated with the SelectScreen®.

3.3. Antiproliferative activity

To test the anticancer activity of the synthesized compounds, we evaluated the antiproliferative activities of several compounds against MDA-MB-231 (human breast cancer cell) and A549 (human lung cancer cell) cell lines, in which FAK has been found to be overexpressed [28,29], using the MTT assay. TAE-226 was tested for comparison. As shown in Table 7, most of the target compounds possessed significant anticancer activities with IC_{50} values ranging from 0.5 to 17.7 μM. As a general trend, most of the compounds exhibited less than 15 μM antiproliferative activities against MDA-MB-231 cells, and six of the compounds (**11d**, **20b**, **20l**, **22b**, **22d**, **25h**) showed antiproliferative activities against MDA-MB-231 cells similar to those of TAE-226. Three compounds (**20b**, **20l**, **25h**) displayed significant potency to A549 cells with IC_{50} values of 0.5−2.0 μM. In addition, normal human cell line HK2 (normal human tubular epithelial cell) was also used to test their cytotoxicity. These compounds also showed low cytotoxicity toward the normal HK2 cells, indicating that these compounds exert less effect on HK2 cells than the cancer cells.

3.4. Effects of compound *25b* on cell apoptosis

To investigate the antiproliferative mechanism of **25b** on A549 cells, the effects of **25b** on apoptosis in A549 cells were tested by flow cytometry. A549 cells were incubated with DMSO and **25b** (1, 3 and 9 μM) for 72 h. As shown in Fig. 4. Compound **25b** strongly induced apoptosis of A549 cells in a concentration-dependent manner with apoptotic rates of 22.89%, 42.39%, and 66.71% at concentrations of 1, 3 and 9 μM, respectively.

Table 7
Antiproliferative activity of several compounds.

Compd.	MDA-MB-231 (μM)[a]	A549 (μM)[a]	HK2 (μM)[a]
11d	4.17 ± 0.18	3.45 ± 0.23	9.16 ± 0.18
20b	1.31 ± 0.01	1.02 ± 0.09	4.77 ± 0.38
20d	17.76 ± 1.06	2.93 ± 0.17	>25
20e	6.53 ± 0.51	3.72 ± 0.53	9.75 ± 0.93
20h	12.41 ± 0.60	2.48 ± 0.25	>25
20i	8.80 ± 1.14	9.88 ± 0.06	>25
20j	14.30 ± 0.43	9.80 ± 0.22	8.89 ± 0.37
20l	4.35 ± 0.29	0.53 ± 0.04	8.33 ± 0.18
22b	3.43 ± 0.15	7.53 ± 0.22	4.40 ± 0.91
22c	8.18 ± 0.47	17.40 ± 1.53	>25
22d	5.53 ± 0.27	7.01 ± 0.22	14.42 ± 2.09
22e	14.11 ± 0.12	14.53 ± 1.27	>25
25b	17.41 ± 1.53	3.20 ± 0.41	>25
25f	11.29 ± 0.59	2.24 ± 0.47	>25
25h	4.17 ± 0.24	1.61 ± 0.16	21.88 ± 3.13
TAE-226	4.24 ± 0.034	1.02 ± 0.14	8.20 ± 1.01

[a] Concentration that inhibits the proliferation of cancer cells by 50%. Cell proliferation was determined by MTT assay after incubation with compounds for 72 h. The mean values of three independent experiments ± SE are reported.

3.5. Effects of compound *25b* on cell migration

To further investigate the effect of **25b** on the migration of A549 cells, transwell assays were performed. A549 cells were incubated with DMSO and **25b** (1, 3 and 9 μM) for 72 h. Under these conditions, as displayed in Fig. 5A and B, the number of cells that permeated the membrane were reduced in a concentration-dependent manner. These results demonstrated that **25b** has a significant anti-metastatic ability against A549 cells.

3.6. In vitro metabolic stability and CYP450 inhibition of compound *25b*

We investigated the *in vitro* metabolic stability of compound **25b** in mouse, rat and human liver microsomes and we evaluated its ability to inhibit human cytochrome P450 *in vitro*. As shown in Table 8 and Table 9, compound **25b** possessed good microsomal metabolic stability, and it had weak inhibitory effect on CYP1A2, CYP2C9, CYP2C19, CYP2D6 and CYP3A4 metabolism.

3.7. Molecular modeling analysis

To elucidate the interaction mode of compound **25b**, a docking study of this compound in the ATP-binding site of FAK (PDB entry 2JKK) was performed. The predicted binding mode is shown in Fig. 6. The compound is anchored to the hinge region via the canonical donor-acceptor-donor hydrogen bonding motif between the nitrogen molecules on the 7*H*-pyrrolo[2,3-*d*]pyrimidine-2,4-diamine moiety and the backbone of residues Glu500 and Gly502. Further stabilization may be achieved through the hydrophobic interactions of the 7*H*-pyrrolo[2,3-*d*]pyrimidine ring with the hydrophobic side chains of Ala452 and Leu553. The DMPO moiety interacts with Asp564 of the DFG motif via hydrogen bonding. The o-methoxy on the benzene ring occupies the lower hinge area pocket and hydrophobically interacts with the side chain of Leu501. Furthermore, the piperidine moiety points toward the solvent region by forming a hydrogen bond with Cys427 located at the edge of the active pocket.

4. Conclusions

In conclusion, based on a structure-based design approach, a series of 7*H*-pyrrolo[2,3-*d*]pyrimidine derivatives possessing a dimethylphosphine oxide moiety were designed and synthesized. The structure-activity relationship of these compounds was discussed from the perspective of enzymatic and cellular activities. Most compounds potently suppressed the enzymatic activities of FAK with IC_{50} values in the 10^{-8}–10^{-9} M range and potently inhibited the proliferation of breast (MDA-MB-231) and lung (A549) cancer cell lines. In particular, the representative compound

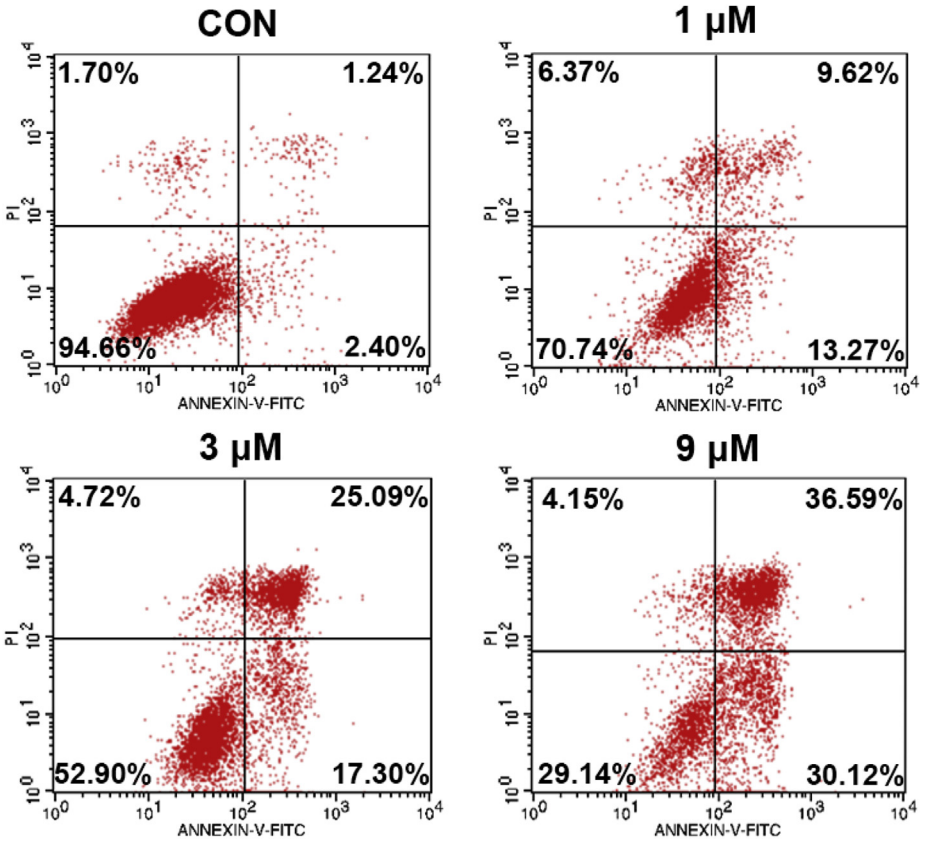

Fig. 4. Effects of compound **25b** on A549 cells apoptosis.

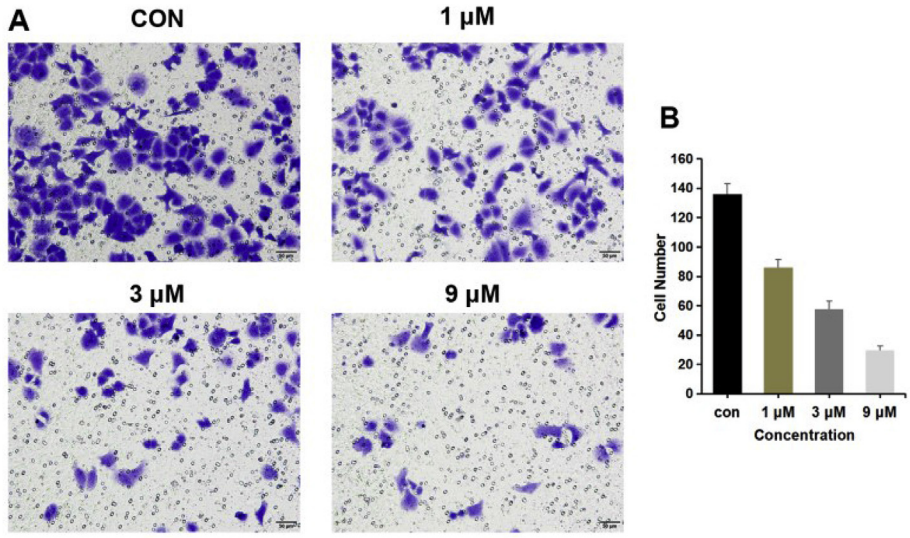

Fig. 5. (A). The effect of compound 25b on the migration of A549 cells were investigated by transwell assays. (B). Quantitative analysis of migration.

Table 8
Liver microsomal stability.

parameters	$T_{1/2}$ (min)	Remaining (%) T = 1 h	Remaining[a] (%) T = 1 h	$CL_{int(mic)}$ (μL/min/mg)	$CL_{int(liver)}$ (mL/min/kg)
in mouse	137.6	75.4	78.0	10.1	39.9
in rat	>145	80.7	76.3	<9.6	<17.3
in human	107.6	67.9	81.2	12.9	11.6

[a] The NADPH regeneration system (replaced with buffer) was not added to the sample during the 1 h incubation.

Table 9
Cytochrome P450 inhibition.[a].

isozyme	CYP1A2	CYP2C9	CYP2C19	CYP2D6	CYP3A4
%inhibition at 10 μM	1.5	11.5	4.9	10.7	10.5

[a] Assays were performed in pooled human liver microsomes.

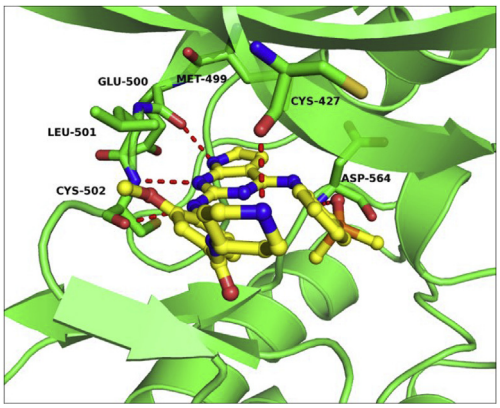

Fig. 6. Predicted binding mode of 25b in the ATP-binding site of FAK. Each dashed red line represents a hydrogen bond. (For interpretation of the references to colour in this figure legend, the reader is referred to the Web version of this article.)

25b exhibited potent enzyme inhibition ($IC_{50} = 5.4$ nM) and good selectivity for a panel of 26 kinases. Furthermore, compound **25b** effectively induced apoptosis and suppressed the migration of A549 cells in a concentration-dependent manner. Further investigation demonstrated that compound **25b** had good metabolic stability in mouse, rat and human liver microsomes *in vitro* and showed weak inhibitory activity against various subtypes of human cytochrome P450. Finally, molecular docking demonstrated the binding pose between compound **25b** and FAK, thereby explaining its anti-FAK activity. Taken together, these results validated the 7*H*-pyrrolo[2,3-*d*]pyrimidine scaffold as a kinase inhibitor platform for designing FAK inhibitors and phosphorus oxide as a hydrogen bond receptor that can be used in drug design. Further investigations on these advanced leads are ongoing and will be reported in the future.

5. Experimental section

5.1. Chemistry

Starting materials, reagents and solvents were obtained from commercial suppliers and used without further purification unless otherwise indicated. Anhydrous solvents were dried and stored according to standard procedures. All reactions were monitored by thin-layer chromatography (TLC) on silica gel plates with fluorescence F-254 and visualized with UV light. Column chromatography was performed on silica gel (200–300 mesh). ^{1}H NMR, ^{13}C NMR and DEPT spectral data were recorded in DMSO-d_6 or $CDCl_3$ on Bruker ARX-600 NMR or Bruker ARX-400 NMR spectrometers with TMS as an internal standard. IR spectra were recorded on a Bruker IFS 55 spectrometer. High-resolution accurate mass spectrometry (HRMS) determinations for all final target compounds were obtained on a Bruker micromass time of flight mass spectrometer equipped with an electrospray ionization (ESI) detector. All melting points were obtained on a Büchi melting point B-540 apparatus and are uncorrected.

5.1.1. Preparation of 2,4-dichloro-7-tosyl-7H-pyrrolo[2,3-d] pyrimidine (**8**)

NaH (1.1 equiv) was slowly added at 0 °C to a 2,4-dichloro-7*H*-pyrrolo[2,3-*d*]pyrimidine (1 equiv) solution in THF. The reaction mixture was stirred at 0 °C for 0.5 h. *p*-Toluensulfonyl chloride (1 equiv) was then added and it was stirred at 0 °C for 4 h. The solvent was evaporated to dryness, and the crude product was diluted with H_2O and extracted thrice with CH_2Cl_2. The organic layer was washed with brine, dried over anhydrous Na_2SO_4, and filtered. The filtrate was concentrated to obtain the crude product for the next step.

5.1.2. General procedure for the synthesis of intermediates **9a-d**

To a solution of **8** (1 equiv) in n-BuOH (20 mL), corresponding amines (1.1 equiv) and *N*-ethyl-*N*-isopropylpropan-2-amine (1.2 equiv) were added. The mixture was stirred at 100 °C for 5 h. The mixture was diluted with EtOAc and washed successively with water and brine. The organic layer was dried over Na_2SO_4, filtered, and evaporated. The resulting intermediate was purified by chromatography.

*5.1.2.1. 2-((2-Chloro-7-tosyl-7H-pyrrolo[2,3-d]pyrimidin-4-yl) amino)-N-methylbenzamide (**9a**).* ^{1}H NMR (600 MHz, DMSO-d_6) δ 11.88 (s, 1H), 8.73 (d, $J = 4.4$ Hz, 1H), 8.30 (d, $J = 8.2$ Hz, 1H), 7.99 (d, $J = 8.4$ Hz, 2H), 7.76–7.72 (m, 2H), 7.57–7.53 (m, 1H), 7.48 (d, $J = 8.3$ Hz, 2H), 7.20 (t, $J = 7.5$ Hz, 1H), 6.75 (d, $J = 3.9$ Hz, 1H), 2.76 (d, $J = 4.5$ Hz, 3H), 2.37 (s, 3H).

*5.1.2.2. (2-((2-Chloro-7-tosyl-7H-pyrrolo[2,3-d]pyrimidin-4-yl) amino)phenyl)dimethylphosphine oxide (**9b**).* ^{1}H NMR (600 MHz, DMSO-d_6) δ 12.37 (s, 1H), 8.59 (dd, $J = 8.3$, 3.8 Hz, 1H), 7.99 (d, $J = 8.4$ Hz, 2H), 7.75 (d, $J = 3.9$ Hz, 1H), 7.65 (dd, $J = 13.7$, 7.6 Hz, 1H), 7.59 (t, $J = 7.9$ Hz, 1H), 7.47 (d, $J = 8.2$ Hz, 2H), 7.18 (t, $J = 7.3$ Hz, 1H), 6.69 (d, $J = 3.7$ Hz, 1H), 2.37 (s, 3H), 1.82 (d, $J = 13.7$ Hz, 6H).

*5.1.2.3. N-(2-(((2-chloro-7-tosyl-7H-pyrrolo[2,3-d]pyrimidin-4-yl) amino)methyl)phenyl)-N-methylmethanesulfonamide (**9c**).* ^{1}H NMR (600 MHz, $CDCl_3$) δ 8.06 (d, $J = 8.3$ Hz, 2H), 7.58 (d, $J = 6.5$ Hz, 1H), 7.36–7.28 (m, 5H), 6.62 (s, 1H), 6.37 (d, $J = 3.7$ Hz, 1H), 5.17 (s, 1H), 4.43 (s, 1H), 3.29 (s, 3H), 3.03 (s, 3H), 2.39 (s, 3H).

*5.1.2.4. 2-((2-Chloro-7-tosyl-7H-pyrrolo[2,3-d]pyrimidin-4-yl) amino)-1-methylpyridin-2(1H)-one (**9d**).* ^{1}H NMR (600 MHz, DMSO-d_6) δ 9.35 (s, 1H), 8.07 (dd, $J = 7.4$, 1.6 Hz, 1H), 7.97 (d, $J = 8.4$ Hz, 2H), 7.69 (d, $J = 4.0$ Hz, 1H), 7.53 (dd, $J = 6.8$, 1.7 Hz, 1H), 7.47 (d, $J = 8.2$ Hz, 2H), 7.14 (d, $J = 3.8$ Hz, 1H), 6.32 (t, $J = 7.1$ Hz, 1H), 3.52 (s, 3H), 2.36 (s, 3H).

5.1.3. General procedure for the synthesis of compounds **10a-h**

To solutions of **9a-d** (1 equiv), corresponding substituted anilines (1.1 equiv), X-phos (0.1 equiv) and Cs_2CO_3 (3.0 equiv) in 1,4-dioxane, $Pd(AcO)_2$ (0.05 equiv) was added under a nitrogen atmosphere. The mixture was purged with nitrogen for 5 min and then heated at 90 °C until completion of the reaction. The mixture was diluted with ethyl acetate, and the organic layer was washed with brine, dried over anhydrous Na_2SO_4 and filtered. The filtrate was concentrated and purified by chromatography to give the coupling intermediates **10a-h**.

5.1.4. General procedure for the synthesis of compounds **11a-h**

Intermediates **10a-h** were dissolved in methanol (5 mL), and a 2 N sodium hydroxide solution (1.0 mL) was added to the mixture. The mixture was heated to 40 °C and stirred for 10 h. The majority of the solvent was removed under vacuum, and the residue was partitioned between ethyl acetate and water. The organic layer was

dried over anhydrous Na_2SO_4 and concentrated. The residue was purified by column chromatography to afford compounds **11a-h**.

*5.1.4.1. 2-((2-((2-Methoxy-4-morpholinophenyl)amino)-7H-pyrrolo[2,3-d]pyrimidin-4-yl)amino)-N-methylbenzamide (**11a**).* White solid; yield: 73%; mp: 233.2–234.0 °C; ^{1}H NMR (600 MHz, DMSO-d_6) δ 11.66 (s, 1H), 11.29 (s, 1H), 8.88 (d, J = 8.3 Hz, 1H), 8.74 (d, J = 4.4 Hz, 1H), 7.96 (d, J = 8.4 Hz, 1H), 7.74 (d, J = 7.8 Hz, 1H), 7.48–7.40 (m, 2H), 7.04 (t, J = 7.5 Hz, 1H), 6.95 (dd, J = 3.1, 2.4 Hz, 1H), 6.66 (d, J = 2.3 Hz, 1H), 6.50 (dd, J = 8.7, 2.3 Hz, 1H), 6.29 (dd, J = 3.0, 1.8 Hz, 1H), 3.83 (s, 3H), 3.77–3.75 (m, 4H), 3.11–3.09 (m, 4H), 2.83 (d, J = 4.5 Hz, 3H). ^{13}C NMR (150 MHz, DMSO-d_6) δ 169.48, 156.31, 152.90, 152.53, 150.34, 147.19, 141.11, 131.74, 127.89, 122.37, 122.00, 120.44, 120.35, 119.86, 118.93, 106.65, 99.98, 98.74, 97.24, 66.21 (2C), 55.58, 49.47 (2C), 26.30. IR (thin film, cm^{-1}) 3435.8, 3323.6, 2922.0, 2852.4, 1617.7, 1580.8, 1522.6, 1446.6, 1398.6, 1225.0, 739.5. HRMS calcd for $C_{25}H_{27}N_7O_3$, $[M+H]^+$, 474.2248; found 474.2253.

*5.1.4.2. N-methyl-2-((2-((4-(methylcarbamoyl)phenyl)amino)-7H-pyrrolo[2,3-d]pyrimidin-4-yl)amino)benzamide (**11b**).* White solid; yield: 78%; mp: 267.9–268.8 °C; ^{1}H NMR (600 MHz, DMSO-d_6) δ 11.75 (s, 1H), 11.48 (s, 1H), 9.31 (s, 1H), 9.03 (d, J = 8.3 Hz, 1H), 8.76 (d, J = 4.5 Hz, 1H), 8.20 (d, J = 4.5 Hz, 1H), 7.91 (d, J = 8.8 Hz, 2H), 7.79–7.74 (m, 3H), 7.53 (t, J = 8.4 Hz, 1H), 7.10–7.05 (m, 2H), 6.35 (dd, J = 3.3, 1.9 Hz, 1H), 2.84 (d, J = 4.5 Hz, 3H), 2.78 (d, J = 4.5 Hz, 3H). ^{13}C NMR (150 MHz, DMSO-d_6) δ 169.52, 166.45, 154.97, 152.88, 151.91, 144.24, 141.01, 131.82, 127.96, 127.61 (2C), 125.75, 120.65, 120.63 (2C), 119.19, 116.96 (2C), 99.40, 97.39, 26.33, 26.16. IR (thin film, cm^{-1}) 3417.9, 2922.0, 2852.1, 1611.4, 1539.0, 1583.0, 1517.5, 1446.9, 1384.9, 1329.7, 751.8. HRMS calcd for $C_{22}H_{21}N_7O_2$, $[M+H]^+$, 416.1830; found 416.1830; $[M+Na]^+$, 438.1649; found 438.1651.

*5.1.4.3. (2-((2-((2-Methoxy-4-(piperazin-1-yl)phenyl)amino)-7H-pyrrolo[2,3-d]pyrimidin-4-yl)amino)phenyl)dimethylphosphine oxide (**11c**).* White solid; yield: 73%; mp: 238.0–239.1 °C; ^{1}H NMR (600 MHz, $CDCl_3$) δ 11.08 (s, 1H), 9.59 (s, 1H), 8.96 (dd, J = 8.4, 4.3 Hz, 1H), 8.26 (d, J = 8.6 Hz, 1H), 7.50 (t, J = 7.9 Hz, 1H), 7.24 (dd, J = 14.2, 7.6 Hz, 1H), 7.16 (s, 1H), 7.04 (t, J = 7.4 Hz, 1H), 6.68 (d, J = 3.4 Hz, 1H), 6.57 (d, J = 2.3 Hz, 1H), 6.53 (dd, J = 8.7, 2.3 Hz, 2H), 3.92–3.88 (m, 7H), 3.14–3.11 (m, 4H), 1.84 (d, J = 13.1 Hz, 6H). ^{13}C NMR (150 MHz, DMSO-d_6) δ 156.28, 153.15, 152.31, 150.42, 147.24, 145.06, 132.29, 130.76 (d, J = 11.4 Hz), 122.35, 122.16, 120.76 (d, J = 12.0 Hz), 120.26 (d, J = 6.3 Hz), 118.18 (d, J = 92.2 Hz), 117.88, 106.65, 99.99, 98.78, 97.90, 66.21 (2C), 55.58, 49.46 (2C), 18.58 (d, J = 70.8 Hz, 2C). IR (thin film, cm^{-1}) 3437.2, 2921.7, 2851.7, 1605.0, 1576.5, 1524.5, 1442.0, 1385.2, 1302.0, 1121.7, 755.9. HRMS calcd for $C_{25}H_{29}N_6O_3P$, $[M+H]^+$, 493.2112; found 493.2116.

*5.1.4.4. 4-((4-((2-(Dimethylphosphoryl)phenyl)amino)-7H-pyrrolo[2,3-d]pyrimidin-2-yl)amino)-N-methylbenzamide (**11d**).* White solid; yield: 76%; mp: 187.7–188.6 °C; ^{1}H NMR (600 MHz, DMSO-d_6) δ 11.69 (s, 1H), 11.44 (s, 1H), 9.32 (s, 1H), 9.11 (dd, J = 7.4, 3.1 Hz, 1H), 8.22 (d, J = 4.0 Hz, 1H), 7.92 (d, J = 8.2 Hz, 2H), 7.77 (d, J = 8.2 Hz, 2H), 7.61–7.53 (m, 2H), 7.10 (t, J = 7.1 Hz, 1H), 7.01 (s, 1H), 6.41 (s, 1H), 2.79 (d, J = 4.1 Hz, 3H), 1.85 (d, J = 13.5 Hz, 6H). ^{13}C NMR (150 MHz, DMSO-d_6) δ 166.42, 154.95, 153.12, 151.76, 145.01, 144.26, 132.37, 130.87 (d, J = 11.0 Hz), 127.59 (2C), 125.73, 120.96 (d, J = 11.8 Hz), 120.40 (d, J = 6.6 Hz), 120.18, 118.35 (d, J = 91.7 Hz), 116.96 (2C), 99.44, 98.02, 26.15, 18.62 (d, J = 70.4 Hz, 2C). Its ^{13}C NMR and DEPT spectrum displayed 22 carbon resonances for 3 primary carbon (δ_C 26.15, 18.62 × 2), 10 tertiary carbon (δ_C 132.37, 130.87, 127.59 × 2, 120.96, 120.40, 120.18, 116.96 × 2, 98.02), 9 quaternary carbon (δ_C 166.42, 154.95, 153.12, 151.76, 145.01, 144.26, 125.73, 118.35, 99.44). IR (thin film, cm^{-1}) 3425.6, 2921.1, 1608.8, 1500.7, 1442.0, 1385.3, 1305.7, 1243.7, 866.3, 755.5. HRMS calcd for $C_{22}H_{23}N_6O_2P$, $[M+H]^+$, 435.1693; found 435.1686; $[M+Na]^+$, 457.1512; found 457.1508.

*5.1.4.5. N-(2-(((2-((2-methoxy-4-morpholinophenyl)amino)-7H-pyrrolo[2,3-d]pyrimidin-4-yl)amino)methyl)phenyl)-N-methylmethanesulfonamide (**11e**).* Grey solid; yield: 82%; mp: 153.4–154.6 °C; ^{1}H NMR (600 MHz, DMSO-d_6) δ 11.05 (s, 1H), 8.18 (d, J = 8.5 Hz, 1H), 7.77 (s, 1H), 7.55–7.50 (m, 1H), 7.41 (dd, J = 6.9, 1.8 Hz, 1H), 7.37–7.28 (m, 2H), 6.94 (s, 1H), 6.78 (s, 1H), 6.61 (d, J = 2.1 Hz, 1H), 6.45 (s, 1H), 6.36 (dd, J = 8.5, 1.6 Hz, 1H), 4.92 (s, 1H), 4.62 (s, 1H), 3.82 (s, 3H), 3.78–3.67 (m, 4H), 3.28 (s, 3H), 3.12 (s, 3H), 3.07–2.95 (m, 4H). ^{13}C NMR (150 MHz, DMSO-d_6) δ 156.36, 155.78, 151.58, 148.15, 145.69, 140.45, 139.64, 128.26, 128.17, 127.68, 126.99, 123.28, 118.53, 118.04, 106.86, 99.99, 98.93, 97.31, 66.21 (2C), 55.66, 49.64 (2C), 40.05, 38.69, 36.13. IR (thin film, cm^{-1}) 3415.1, 2923.2, 2852.7, 1591.1, 1497.0, 1396.8, 1331.4, 1252.8, 1141.5, 1116.6, 731.4. HRMS calcd for $C_{26}H_{31}N_7O_4S$, $[M+H]^+$, 538.2231; found 538.2228.

*5.1.4.6. N-methyl-4-((4-((2-(N-methylmethylsulfonamido)benzyl)amino)-7H-pyrrolo[2,3-d]pyrimidin-2-yl)amino)benzamide (**11f**).* White solid; yield: 85%; mp: 178.0–179.1 °C; ^{1}H NMR (600 MHz, DMSO-d_6) δ 11.14 (s, 1H), 8.91 (s, 1H), 8.12 (dd, J = 8.8, 4.3 Hz, 1H), 7.79 (d, J = 8.7 Hz, 2H), 7.72 (s, 1H), 7.62 (d, J = 8.8 Hz, 2H), 7.54 (dd, J = 7.6, 1.3 Hz, 1H), 7.42 (dd, J = 7.3, 1.5 Hz, 1H), 7.37–7.31 (m, 2H), 6.84 (dd, J = 3.0, 2.5 Hz, 1H), 6.48 (s, 1H), 4.91 (s, 1H), 4.83 (s, 1H), 3.24 (s, 3H), 3.13 (s, 3H), 2.75 (d, J = 4.5 Hz, 3H). ^{13}C NMR (150 MHz, DMSO-d_6) δ 166.48, 156.54, 155.39, 151.38, 144.64, 140.64, 139.74, 128.36, 128.28, 127.81, 127.51 (2C), 127.02, 125.14, 118.59, 116.46 (2C), 99.00, 97.69, 38.79, 36.12, 26.11. IR (thin film, cm^{-1}) 3424.2, 2922.8, 2852.4, 1615.2, 1464.2, 1384.9, 1319.7, 1242.1, 1137.7, 848.9, 729.2. HRMS calcd for $C_{23}H_{25}N_7O_3S$, $[M+Na]^+$, 502.1632; found 502.1631.

*5.1.4.7. 3-((2-((2-Methoxy-4-morpholinophenyl)amino)-7H-pyrrolo[2,3-d]pyrimidin-4-yl)amino)-1-methylpyridin-2(1H)-one (**11g**).* White solid; yield: 72%; mp: 233.9–234.4 °C; ^{1}H NMR (600 MHz, DMSO-d_6) δ 11.29 (s, 1H), 8.53 (d, J = 7.0 Hz, 1H), 8.21 (s, 1H), 7.86 (d, J = 8.6 Hz, 1H), 7.50 (s, 1H), 7.33 (dd, J = 6.8, 1.5 Hz, 1H), 6.93 (dd, J = 3.2, 2.3 Hz, 1H), 6.66 (d, J = 2.4 Hz, 1H), 6.50 (dd, J = 8.7, 2.4 Hz, 1H), 6.45 (dd, J = 3.3, 1.8 Hz, 1H), 6.24 (t, J = 7.1 Hz, 1H), 3.82 (s, 3H), 3.78–3.73 (m, 4H), 3.56 (s, 3H), 3.12–3.07 (m, 4H). ^{13}C NMR (150 MHz, DMSO-d_6) δ 157.42, 156.44, 152.86, 152.69, 150.91, 147.51, 130.12, 129.34, 122.84, 122.18, 120.60, 119.82, 106.61, 105.57, 100.00, 98.20, 97.40, 66.20 (2C), 55.54, 49.41 (2C), 37.15. IR (thin film, cm^{-1}) 3437.2, 2921.7, 2851.7, 2344.7, 1624.3, 1581.2, 1522.4, 1488.1, 1384.2, 1227.8, 745.5. HRMS calcd for $C_{23}H_{25}N_7O_3$, $[M+H]^+$, 448.2092; found 448.2097.

*5.1.4.8. N-methyl-4-((4-((1-methyl-2-oxo-1,2-dihydropyridin-3-yl)amino)-7H-pyrrolo[2,3-d]pyrimidin-2-yl)amino)benzamide (**11h**).* White solid; yield: 78%; mp: 283.0–284.5 °C; ^{1}H NMR (600 MHz, DMSO-d_6) δ 11.50 (s, 1H), 9.33 (s, 1H), 8.75 (dd, J = 7.4, 1.4 Hz, 1H), 8.34 (s, 1H), 8.20 (q, J = 4.1 Hz, 1H), 7.91 (d, J = 8.8 Hz, 2H), 7.76 (d, J = 8.8 Hz, 2H), 7.38 (dd, J = 6.8, 1.6 Hz, 1H), 7.04 (dd, J = 3.4, 2.3 Hz, 1H), 6.54 (dd, J = 3.4, 1.9 Hz, 1H), 6.33 (t, J = 7.1 Hz, 1H), 3.58 (s, 3H), 2.78 (d, J = 4.5 Hz, 3H). ^{13}C NMR (150 MHz, DMSO-d_6) δ 166.44, 157.50, 154.84, 152.87, 151.96, 144.18, 130.47, 129.29, 127.63 (2C), 125.81, 121.07, 120.61, 116.92 (2C), 105.59, 98.93, 97.66, 37.19, 26.16. IR (thin film, cm^{-1}) 3424.3, 2922.5, 2852.5, 2344.6, 1626.8, 1511.3, 1475.0, 1384.5, 1324.6, 869.4. HRMS calcd for $C_{20}H_{19}N_7O_2$, $[M+H]^+$, 390.1673; found 390.1672.

*5.1.5. Preparation of N-(2-(aminomethyl)phenyl)-N-methylmethanesulfonamide (**14**)*

To a solution of 2-fluoro-benzonitrile (1 equiv), *N*-Methylmethanesulfonamide (1 equiv), and cesium carbonate (1.2 equiv) in acetonitrile. The reaction mixture was stirred at 80 °C for 10 h. Upon completion, the mixture was filtered and then concentrated. The residue was diluted with water and extracted by CH_2Cl_2. The organic phases were combined, washed by brine, dried over anhydrous Na_2SO_4 and evaporated to afford crude product **13**. Intermediate **13** (1 equiv) was dissolved in anhydrous tetrahydrofuran and protected with argon. BH_3 (in 2M THF) (1.5 equiv) was then added, and the mixture was stirred at 70 °C until completion of the reaction. The reaction was quenched with H_2O and extracted thrice with CH_2Cl_2, and the organic layer was washed with brine, dried over anhydrous Na_2SO_4, and filtered. The filtrate was concentrated and purified by chromatography to afford intermediate **14**.

*5.1.6. Preparation of 3-amino-1-methylpyridin-2(1H)-one (**17**)*

NaH (1.1 equiv) was slowly added at 0 °C to a 3-nitropyridin-2(1*H*)-one (1 equiv) solution in THF. The reaction mixture was stirred at 0 °C for 0.5 h. Iodomethane (1 equiv) was then added and the mixture was stirred at 55 °C for 6 h. The reaction was diluted with H_2O and extracted thrice with EA, and the organic layer was washed with brine, dried over anhydrous Na_2SO_4, filtered and concentrated to afford crude product **16**. Intermediate **16** (1 equiv) was dissolved in methanol, and Pd/C (0.1 equiv) was added. The flask was flushed with H_2 and stirred for 5 h at 40 °C. The reaction mixture was filtered, concentrated and purified by chromatography to afford intermediate **17**.

*5.1.7. Preparation of compounds **20a-l**, **22a-g** and **25a-h***

Compounds **20a-l**, **22a-g** and **25a-h** were prepared in a similar manner as compounds **11a-h**.

*5.1.7.1. N-(4-((4-((2-(dimethylphosphoryl)phenyl)amino)-7H-pyrrolo[2,3-d]pyrimidin-2-yl)amino)phenyl)acetamide (**20a**).* White solid; yield: 73%; mp: 217.9–218.5 °C; ^{1}H NMR (600 MHz, DMSO-d_6) δ 11.62 (s, 1H), 11.26 (s, 1H), 9.77 (s, 1H), 9.11 (dd, *J* = 8.3, 3.9 Hz, 1H), 8.89 (s, 1H), 7.71 (d, *J* = 8.8 Hz, 2H), 7.56 (dd, *J* = 13.7, 7.6 Hz, 1H), 7.51–7.43 (m, 3H), 7.06 (t, *J* = 7.3 Hz, 1H), 6.94–6.92 (m, 1H), 6.36 (dd, *J* = 3.1, 1.9 Hz, 1H), 2.02 (s, 3H), 1.83 (d, *J* = 13.5 Hz, 6H). ^{13}C NMR (150 MHz, DMSO-d_6) δ 167.63, 155.68, 153.10, 152.16, 145.15, 137.09, 132.44, 132.28, 130.80 (d, *J* = 11.5 Hz), 120.74 (d, *J* = 12.1 Hz), 120.36 (d, *J* = 6.2 Hz), 119.56, 119.46 (2C), 118.94 (2C), 118.12 (d, *J* = 91.9 Hz), 98.93, 97.95, 23.83, 18.63 (d, *J* = 70.7 Hz, 2C). IR (thin film, cm^{-1}) 3437.1, 2921.6, 2851.9, 1637.0, 1384.5, 1122.4, 573.3. HRMS calcd for $C_{22}H_{23}N_6O_2P$, $[M+H]^+$, 435.1693; found 435.1693; $[M+Na]^+$, 457.1512; found 457.1515.

*5.1.7.2. 4-((4-((2-(dimethylphosphoryl)phenyl)amino)-7H-pyrrolo[2,3-d]pyrimidin-2-yl)amino)-N-ethylbenzenesulfonamide (**20b**).* White solid; yield: 83%; mp: 276.1–277.0 °C; ^{1}H NMR (600 MHz, DMSO-d_6) δ 11.71 (s, 1H), 11.46 (s, 1H), 9.51 (s, 1H), 9.07 (dd, *J* = 8.4, 4.0 Hz, 1H), 8.01 (d, *J* = 8.8 Hz, 2H), 7.65 (d, *J* = 8.8 Hz, 2H), 7.59 (dd, *J* = 14.0, 7.6 Hz, 1H), 7.53 (t, *J* = 7.8 Hz, 1H), 7.30 (t, *J* = 5.8 Hz, 1H), 7.10 (t, *J* = 7.2 Hz, 1H), 7.04–7.02 (m, 1H), 6.41 (dd, *J* = 3.1, 1.9 Hz, 1H), 2.80–2.73 (m, 2H), 1.84 (d, *J* = 13.5 Hz, 6H), 0.98 (t, *J* = 7.2 Hz, 3H). ^{13}C NMR (150 MHz, DMSO-d_6) δ 154.65, 153.15, 151.57, 145.22, 144.90, 132.32, 130.91 (d, *J* = 11.2 Hz), 130.64, 127.33 (2C), 121.09 (d, *J* = 12.0 Hz), 120.49, 120.45, 118.55 (d, *J* = 91.7 Hz), 117.33 (2C), 99.69, 98.05, 37.48, 18.61 (d, *J* = 70.8 Hz, 2C), 14.68. IR (thin film, cm^{-1}) 3425.3, 3332.7, 2922.1, 2852.5, 1631.0, 1579.7, 1579.7, 1479.1, 1439.2, 1302.0, 869.3, 741.9. HRMS calcd for $C_{22}H_{25}N_6O_3PS$, $[M+Na]^+$, 507.1339; found 507.1348.

*5.1.7.3. Dimethyl(4-((4-((2-(dimethylphosphoryl)phenyl)amino)-7H-pyrrolo[2,3-d]pyrimidin-2-yl)amino)benzyl)phosphonate (**20c**).* White solid; yield: 77%; mp: 158.3–159.1 °C; ^{1}H NMR (600 MHz, DMSO-d_6) δ 11.63 (s, 1H), 11.31 (s, 1H), 9.11 (dd, *J* = 8.3, 4.0 Hz, 1H), 8.96 (s, 1H), 7.74 (d, *J* = 8.3 Hz, 2H), 7.57 (ddd, *J* = 14.1, 7.7, 1.1 Hz, 1H), 7.51 (t, *J* = 7.9 Hz, 1H), 7.17 (dd, *J* = 8.6, 2.2 Hz, 2H), 7.07 (t, *J* = 7.3 Hz, 1H), 6.95 (dd, *J* = 3.3, 2.3 Hz, 1H), 6.37 (dd, *J* = 3.4, 2.0 Hz, 1H), 3.61 (s, 3H), 3.60 (s, 3H), 3.21 (s, 1H), 3.17 (s, 1H), 1.83 (d, *J* = 13.5 Hz, 6H). ^{13}C NMR (150 MHz, DMSO-d_6) δ 155.55, 153.11, 152.08, 145.14, 140.18 (d, *J* = 3.1 Hz), 132.33, 130.81 (d, *J* = 11.4 Hz), 129.53 (d, *J* = 6.5 Hz, 2C), 123.23 (d, *J* = 9.0 Hz), 120.78 (d, *J* = 12.1 Hz), 120.36 (d, *J* = 6.5 Hz), 119.69, 118.72 (d, *J* = 3.2 Hz, 2C), 118.13 (d, *J* = 91.8 Hz), 99.05, 97.95, 52.30 (d, *J* = 6.6 Hz, 2C), 30.43 (d, *J* = 135.4 Hz), 18.63 (d, *J* = 70.5 Hz, 2C). IR (thin film, cm^{-1}) 3423.0, 2922.1, 2852.1, 1602.0, 1579.5, 1518.8, 1441.5, 1385.2, 1306.9, 866.2, 757.2. HRMS calcd for $C_{23}H_{27}N_5O_4P_2$, $[M+Na]^+$, 522.1430; found 522.1435.

*5.1.7.4. 2-((4-((2-(Dimethylphosphoryl)phenyl)amino)-7H-pyrrolo[2,3-d]pyrimidin-2-yl)amino)-N-(piperidin-4-yl)benzamide (**20d**).* White solid; yield: 89%; mp: 223.3–224.0 °C; ^{1}H NMR (400 MHz, DMSO-d_6) δ 11.68 (s, 1H), 11.42 (s, 1H), 9.31 (s, 1H), 9.11 (dd, *J* = 8.3, 4.1 Hz, 1H), 8.15 (d, *J* = 7.4 Hz, 1H), 7.93 (d, *J* = 8.7 Hz, 2H), 7.80 (d, *J* = 8.7 Hz, 2H), 7.62–7.50 (m, 2H), 7.09 (t, *J* = 7.1 Hz, 1H), 7.01 (d, *J* = 0.9 Hz, 1H), 6.41 (d, *J* = 1.9 Hz, 1H), 4.01–3.95 (m, 1H), 3.22 (d, *J* = 12.5 Hz, 2H), 2.87 (t, *J* = 11.2 Hz, 2H), 1.91 (d, *J* = 11.1 Hz, 2H), 1.84 (d, *J* = 13.5 Hz, 6H), 1.65 (dd, *J* = 21.4, 11.1 Hz, 2H). ^{13}C NMR (150 MHz, DMSO-d_6) δ 165.56, 154.93, 153.14, 151.72, 145.04, 144.47, 132.40, 130.89 (d, *J* = 11.2 Hz), 127.99 (2C), 125.59, 120.99 (d, *J* = 12.1 Hz), 120.40 (d, *J* = 6.5 Hz), 120.23, 118.34 (d, *J* = 91.8 Hz), 116.80 (2C), 99.49, 98.05, 45.18, 43.33 (2C), 29.87 (2C), 18.63 (d, *J* = 70.7 Hz, 2C). IR (thin film, cm^{-1}) 3421.0, 2922.3, 2852.1, 1679.5, 1601.8, 1579.2, 1500.7, 1441.1, 1396.1, 1308.8, 867.2, 755.5. HRMS calcd for $C_{26}H_{30}N_7O_2P$, $[M+H]^+$, 504.2271; found 504.2262.

*5.1.7.5. 4-((4-((2-(Dimethylphosphoryl)phenyl)amino)-7H-pyrrolo[2,3-d]pyrimidin-2-yl)amino)-N-(tetrahydro-2H-pyran-4-yl)benzamide (**20e**).* Grey solid; yield: 78%; mp: 230.8–231.5 °C; ^{1}H NMR (600 MHz, DMSO-d_6) δ 11.69 (s, 1H), 11.42 (s, 1H), 9.32 (s, 1H), 9.12 (dd, *J* = 8.3, 3.9 Hz, 1H), 8.07 (d, *J* = 7.7 Hz, 1H), 7.92 (d, *J* = 8.7 Hz, 2H), 7.79 (d, *J* = 8.7 Hz, 2H), 7.59 (dd, *J* = 14.0, 7.7 Hz, 1H), 7.54 (t, *J* = 7.8 Hz, 1H), 7.10 (t, *J* = 7.3 Hz, 1H), 7.02–7.00 (m, 1H), 6.40 (dd, *J* = 3.1, 1.9 Hz, 1H), 4.02–3.98 (m, 1H), 3.89 (d, *J* = 9.3 Hz, 2H), 3.41–3.38 (m, 2H), 1.84 (d, *J* = 13.5 Hz, 6H), 1.75 (dd, *J* = 12.6, 2.2 Hz, 2H), 1.61–1.56 (m, 2H). ^{13}C NMR (150 MHz, DMSO-d_6) δ 165.33, 154.91, 153.14, 151.66, 145.05, 144.37, 132.43, 130.93 (d, *J* = 11.2 Hz), 127.93 (2C), 125.75, 121.00 (d, *J* = 12.1 Hz), 120.38 (d, *J* = 6.3 Hz), 120.24, 118.30 (d, *J* = 91.8 Hz), 116.82 (2C), 99.48, 98.06, 66.29 (2C), 45.59, 32.63 (2C), 18.66 (d, *J* = 70.7 Hz, 2C). IR (thin film, cm^{-1}) 3427.1, 2921.9, 2851.9, 2343.4, 1628.1, 1441.7, 1384.4, 1293.4, 1238.0, 867.1. HRMS calcd for $C_{26}H_{29}N_6O_3P$, $[M+Na]^+$, 527.1931; found 527.1927.

*5.1.7.6. 4-((4-((2-(Dimethylphosphoryl)phenyl)amino)-7H-pyrrolo[2,3-d]pyrimidin-2-yl)amino)-N-(1-methylpiperidin-4-yl)benzamide (**20f**).* White solid; yield: 63%; mp: 230.2–231.0 °C; ^{1}H NMR (600 MHz, DMSO-d_6) δ 11.68 (s, 1H), 11.42 (s, 1H), 9.30 (s, 1H), 9.11 (dd, *J* = 8.3, 3.9 Hz, 1H), 8.01 (d, *J* = 7.7 Hz, 1H), 7.92 (d, *J* = 8.7 Hz, 2H), 7.79 (d, *J* = 8.7 Hz, 2H), 7.58 (dd, *J* = 14.1, 7.7 Hz, 1H), 7.54 (t, *J* = 7.9 Hz, 1H), 7.09 (t, *J* = 7.3 Hz, 1H), 7.00 (dd, *J* = 3.1, 2.4 Hz, 1H), 6.41 (dd, *J* = 3.2, 1.9 Hz, 1H), 3.78–3.71 (m, 1H), 2.81 (d, *J* = 11.4 Hz, 2H), 2.20 (s, 3H), 2.01 (t, *J* = 10.6 Hz, 2H), 1.84 (d, *J* = 13.5 Hz, 6H), 1.77 (d, *J* = 12.1 Hz, 2H), 1.61 (qd, *J* = 12.2, 3.5 Hz, 2H). ^{13}C NMR (150 MHz, DMSO-d_6) δ 165.49, 154.98, 153.17, 151.76, 145.06, 144.37, 132.47, 130.94 (d, *J* = 11.1 Hz), 127.94 (2C), 125.83, 121.04 (d,

J = 12.2 Hz), 120.44 (d, J = 6.4 Hz), 120.26, 118.33 (d, J = 91.8 Hz), 116.84 (2C), 99.50, 98.09, 54.52, 46.25, 45.83 (2C), 31.46 (2C), 18.66 (d, J = 70.9 Hz, 2C). IR (thin film, cm^{-1}) 3423.1, 2921.7, 2851.3, 1631.0, 1499.5, 1440.0, 1384.7, 1308.5, 1242.8, 756.4. HRMS calcd for $C_{27}H_{32}N_7O_2P$, $[M+H]^+$, 518.2428; found 518.2420.

*5.1.7.7. (R)-4-((4-((2-(dimethylphosphoryl)phenyl)amino)-7H-pyrrolo[2,3-d]pyrimidin-2-yl)amino)-N-(piperidin-3-yl)benzamide (**20g**).* White solid; yield: 73%; mp: 273.5–274.2 °C; ^{1}H NMR (600 MHz, DMSO-d_6) δ 11.68 (s, 1H), 11.45 (s, 1H), 9.30 (s, 1H), 9.12 (d, J = 4.2 Hz, 1H), 8.04–7.83 (m, 3H), 7.78 (d, J = 8.6 Hz, 2H), 7.59 (dd, J = 14.1, 7.7 Hz, 1H), 7.54 (t, J = 7.7 Hz, 1H), 7.10 (t, J = 7.2 Hz, 1H), 7.00 (d, J = 3.0 Hz, 1H), 6.40 (d, J = 3.3 Hz, 1H), 3.87–3.61 (m, 2H), 2.99–2.75 (m, 2H), 2.40 (t, J = 10.5 Hz, 1H), 1.84 (d, J = 13.5 Hz, 6H), 1.66–1.38 (m, 3H), 1.28 (dd, J = 13.5, 7.0 Hz, 1H). ^{13}C NMR (150 MHz, DMSO-d_6) δ 165.40, 154.96, 153.14, 151.74, 145.05, 144.31, 132.45, 130.92 (d, J = 11.5 Hz), 127.91 (2C), 125.86, 121.00 (d, J = 11.9 Hz), 120.40 (d, J = 6.2 Hz), 120.23, 118.30 (d, J = 91.9 Hz), 116.81 (2C), 99.46, 98.04, 51.45, 46.82, 45.79, 30.90, 25.58, 18.65 (d, J = 71.0 Hz, 2C). IR (thin film, cm^{-1}) 3427.4, 2921.5, 2851.9, 1634.5, 1440.7, 1384.5, 1308.3, 1125.1, 847.6, 758.5. HRMS calcd for $C_{26}H_{30}N_7O_2P$, $[M+Na]^+$, 526.2091; found 526.2088.

*5.1.7.8. (S)-4-((4-((2-(dimethylphosphoryl)phenyl)amino)-7H-pyrrolo[2,3-d]pyrimidin-2-yl)amino)-N-(piperidin-3-yl)benzamide Hydrochloride(**20h**).* Yellow solid; yield: 78%; mp: 271.3–272.5 °C; ^{1}H NMR (400 MHz, DMSO-d_6) δ 11.88 (s, 1H), 11.79 (s, 1H), 9.87 (s, 1H), 9.47 (d, J = 8.4 Hz, 1H), 9.07 (d, J = 7.1 Hz, 1H), 8.83 (dd, J = 7.8, 3.7 Hz, 1H), 8.54 (d, J = 7.7 Hz, 1H), 7.92 (d, J = 8.8 Hz, 2H), 7.84 (d, J = 8.8 Hz, 2H), 7.65 (dd, J = 13.7, 7.5 Hz, 1H), 7.58 (t, J = 7.8 Hz, 1H), 7.19 (t, J = 7.2 Hz, 1H), 7.05 (dd, J = 3.1, 2.4 Hz, 1H), 6.45 (s, 1H), 4.27–4.23 (m, 1H), 3.28 (d, J = 10.3 Hz, 1H), 3.13 (d, J = 11.3 Hz, 1H), 2.91 (td, J = 19.0, 10.3 Hz, 2H), 1.93–1.87 (m, 2H), 1.83 (d, J = 13.6 Hz, 6H), 1.74–1.65 (m, 2H). ^{13}C NMR (150 MHz, DMSO-d_6) δ 172.04, 165.51, 153.50, 152.74, 143.65, 143.26, 132.57, 131.21 (d, J = 10.8 Hz), 128.33 (2C), 126.39, 122.50 (d, J = 11.6 Hz), 121.70, 120.79, 120.47 (d, J = 94.9 Hz), 117.89 (2C), 99.35, 98.98, 46.25, 43.18, 42.92, 27.96, 20.19, 18.56 (d, J = 70.8 Hz, 2C). IR (thin film, cm^{-1}) 3424.8, 2922.3, 2852.1, 1630.0, 1547.7, 1507.6, 1462.9, 1384.2, 869.8, 761.4. HRMS calcd for $C_{26}H_{30}N_7O_2P$, $[M+H]^+$, 504.2271; found 504.2266.

*5.1.7.9. (4-((4-((2-(dimethylphosphoryl)phenyl)amino)-7H-pyrrolo[2,3-d]pyrimidin-2-yl)amino)phenyl)(piperazin-1-yl)methanone hydrochloride (**20i**).* White solid; yield: 91%; mp: 230.2–231.0 °C; ^{1}H NMR (600 MHz, DMSO-d_6) δ 11.86 (s, 1H), 11.68 (s, 1H), 9.75 (s, 1H), 9.38 (s, 2H), 8.87 (s, 1H), 7.85 (d, J = 8.3 Hz, 2H), 7.64 (dd, J = 13.7, 7.6 Hz, 1H), 7.54 (t, J = 7.8 Hz, 1H), 7.43 (d, J = 8.6 Hz, 2H), 7.17 (t, J = 7.3 Hz, 1H), 7.05–7.02 (m, 1H), 6.44 (s, 1H), 3.75 (s, 4H), 3.16 (s, 4H), 1.83 (d, J = 13.5 Hz, 6H). ^{13}C NMR (150 MHz, DMSO-d_6) δ 172.05, 169.38, 153.73, 152.11, 143.18, 141.46, 132.51, 131.30 (d, J = 10.8 Hz), 128.29 (2C), 127.84, 122.98 (d, J = 11.4 Hz), 122.19, 120.89, 119.05 (2C), 118.04, 99.30, 99.26, 42.50 (2C), 21.12 (2C), 18.52 (d, J = 70.8 Hz, 2C). IR (thin film, cm^{-1}) 3422.7, 2922.1, 2852.3, 2375.3, 1628.7, 1510.6, 1384.3, 1104.8. HRMS calcd for $C_{25}H_{28}N_7O_2P$, $[M+H]^+$, 490.2115; found 490.2111; $[M+Na]^+$, 512.1934; found 512.1938.

*5.1.7.10. (4-((4-((2-(Dimethylphosphoryl)phenyl)amino)-7H-pyrrolo[2,3-d]pyrimidin-2-yl)amino)phenyl)(morpholino)methanone (**20j**).* White solid; yield: 84%; mp: 191.3–192.1 °C; ^{1}H NMR (600 MHz, DMSO-d_6) δ 11.67 (s, 1H), 11.40 (s, 1H), 9.28 (s, 1H), 9.09 (dd, J = 8.3, 3.9 Hz, 1H), 7.92 (d, J = 8.5 Hz, 2H), 7.58 (dd, J = 13.9, 7.7 Hz, 1H), 7.52 (t, J = 7.8 Hz, 1H), 7.35 (d, J = 8.5 Hz, 2H), 7.09 (t, J = 7.3 Hz, 1H), 7.02–6.97 (m, 1H), 6.40 (s, 1H), 3.62 (s, 4H), 3.53 (s, 4H), 1.83 (d, J = 13.5 Hz, 6H). ^{13}C NMR (150 MHz, DMSO-d_6) δ 169.44, 155.04, 153.14, 151.77, 145.00, 143.19, 132.36, 130.86 (d, J = 11.1 Hz), 128.05 (2C), 126.37, 120.97 (d, J = 12.1 Hz), 120.42 (d, J = 6.2 Hz), 120.11, 118.37 (d, J = 91.8 Hz), 117.30 (2C), 99.40, 98.01, 66.16 (2C), 18.61 (d, J = 70.6 Hz, 2C). Its ^{13}C NMR and DEPT spectrum displayed 23 carbon resonances for 2 primary carbon (δ_C 18.61 × 2), 2 secondary carbon (δ_C 66.16 × 2), 10 tertiary carbon (δ_C 132.36, 130.86, 128.05 × 2, 120.97, 120.42, 120.11, 117.30 × 2, 98.01), 9 quaternary carbon (δ_C 169.44, 155.04, 153.14, 151.77, 145.00, 143.19, 126.37, 118.37, 99.40). IR (thin film, cm^{-1}) 3422.3, 2921.8, 2852.7, 1603.6, 1580.0, 1523.8, 1440.5, 1385.4, 1304.4, 867.5, 758.4. HRMS calcd for $C_{25}H_{27}N_6O_3P$, $[M+H]^+$, 491.1954; found 491.1955; $[M+Na]^+$, 513.1774; found 513.1774.

*5.1.7.11. Dimethyl(2-((2-((4-(4-methylpiperazin-1-yl)phenyl)amino)-7H-pyrrolo[2,3-d]pyrimidin-4-yl)amino)phenyl)phosphine oxide (**20k**).* White solid; yield: 77%; mp: 179.1–179.6 °C; ^{1}H NMR (400 MHz, $CDCl_3$) δ 11.11 (s, 1H), 9.66 (s, 1H), 8.94 (dd, J = 8.3, 4.4 Hz, 1H), 7.52–7.43 (m, 3H), 7.21 (dd, J = 14.2, 7.5 Hz, 1H), 7.01 (t, J = 6.6 Hz, 1H), 6.90 (d, J = 8.8 Hz, 2H), 6.86 (s, 1H), 6.57 (d, J = 3.3 Hz, 1H), 6.51 (d, J = 3.2 Hz, 1H), 3.24–3.18 (m, 4H), 2.68 (s, 4H), 2.41 (s, 3H), 1.83 (d, J = 13.1 Hz, 6H). ^{13}C NMR (100 MHz, $CDCl_3$) δ 156.56, 154.06, 152.63, 146.75, 145.64 (d, J = 2.8 Hz), 133.67, 132.93, 129.65 (d, J = 11.2 Hz), 121.99 (2C), 121.70 (d, J = 6.9 Hz), 121.19 (d, J = 12.4 Hz), 119.07, 117.97 (d, J = 89.0 Hz), 117.46 (2C), 99.88, 99.27, 55.01 (2C), 49.80 (2C), 45.81, 18.97 (d, J = 71.6 Hz, 2C). IR (thin film, cm^{-1}) 3422.5, 2922.4, 2851.5, 1638.7, 1602.4, 1515.3, 1439.5, 1385.4, 1291.0, 1123.8, 755.0. HRMS calcd for $C_{25}H_{30}N_7OP$, $[M+H]^+$, 476.2322; found 476.2301.

*5.1.7.12. Dimethyl(2-((2-((4-(piperazin-1-yl)phenyl)amino)-7H-pyrrolo[2,3-d]pyrimidin-4-yl)amino)phenyl)phosphine oxide hydrochloride (**20l**).* White solid; yield: 90%; mp: 284.9–286.0 °C; ^{1}H NMR (400 MHz, DMSO-d_6) δ 12.39 (s, 1H), 12.15 (s, 1H), 10.35 (s, 1H), 9.61 (s, 2H), 8.49 (d, J = 4.0 Hz, 1H), 7.70 (ddd, J = 13.7, 7.7, 1.1 Hz, 1H), 7.50–7.42 (m, 3H), 7.27 (t, J = 7.2 Hz, 1H), 7.10 (d, J = 9.0 Hz, 2H), 7.05 (dd, J = 3.3, 2.3 Hz, 1H), 6.48 (s, 1H), 3.50–3.40 (m, 4H), 3.26 (s, 4H), 1.82 (d, J = 13.7 Hz, 6H). ^{13}C NMR (150 MHz, DMSO-d_6) δ 154.25, 150.59, 146.65, 142.27, 132.47, 131.37 (d, J = 10.5 Hz), 130.56, 123.95 (d, J = 9.2 Hz), 123.67 (2C), 122.51, 120.87, 116.82 (2C), 100.13, 98.82, 46.08 (2C), 42.37 (2C), 18.47 (d, J = 70.6 Hz, 2C). IR (thin film, cm^{-1}) 3428.1, 3100.8, 292.4, 2455.7, 1639.9, 1563.5, 1512.6, 1461.9, 1382.8, 1370.9, 1120.8, 742.9. HRMS calcd for $C_{24}H_{28}N_7OP$, $[M+H]^+$, 462.2166; found 462.2155.

*5.1.7.13. Dimethyl(2-((2-((1-methyl-1H-pyrazol-4-yl)amino)-7H-pyrrolo[2,3-d]pyrimidin-4-yl)amino)phenyl)phosphine oxide (**22a**).* White solid; yield: 72%; mp: 138.2–138.9 °C; ^{1}H NMR (600 MHz, DMSO-d_6) δ 11.52 (s, 1H), 11.16 (s, 1H), 9.07 (s, 1H), 8.77 (s, 1H), 7.90 (s, 1H), 7.57 (dd, J = 13.7, 7.4 Hz, 1H), 7.51 (t, J = 7.6 Hz, 2H), 7.07 (t, J = 7.2 Hz, 1H), 6.89 (dd, J = 3.3, 2.2 Hz, 1H), 6.34 (dd, J = 3.2, 1.9 Hz, 1H), 3.80 (s, 3H), 1.83 (d, J = 13.5 Hz, 6H). ^{13}C NMR (150 MHz, DMSO-d_6) δ 155.70, 153.35, 152.64, 145.23, 132.28, 130.88 (d, J = 11.4 Hz), 129.83, 124.50, 120.82 (d, J = 11.8 Hz), 120.40, 120.09, 119.08, 118.39 (d, J = 92.6 Hz), 98.24, 97.94, 38.66, 18.62 (d, J = 70.7 Hz, 2C). IR (thin film, cm^{-1}) 3421.0, 2922.3, 2852.3, 1631.8, 1578.3, 1438.0, 1385.4, 1291.3, 1124.1, 754.4. HRMS calcd for $C_{18}H_{20}N_7OP$, $[M+H]^+$, 382.1540; found 382.1542; $[M+Na]^+$, 404.1359; found 404.1361.

*5.1.7.14. (2-((2-((1-(2,2-Difluoroethyl)-1H-pyrazol-4-yl)amino)-7H-pyrrolo[2,3-d]pyrimidin-4-yl)amino)phenyl)dimethylphosphine oxide (**22b**).* White solid; yield: 79%; mp: 136.0–136.6 °C; ^{1}H NMR (600 MHz, DMSO-d_6) δ 11.56 (s, 1H), 11.19 (s, 1H), 9.07 (s, 1H), 8.87 (s, 1H), 8.00 (s, 1H), 7.67 (s, 1H), 7.57 (dd, J = 13.9, 7.6 Hz, 1H), 7.51 (t, J = 7.7 Hz, 1H), 7.07 (t, J = 7.2 Hz, 1H), 6.90 (s, 1H), 6.45–6.24 (m,

2H), 4.56 (td, $J = 14.8$, 2.8 Hz, 2H), 1.83 (d, $J = 13.5$ Hz, 6H). ^{13}C NMR (150 MHz, DMSO-d_6) δ 155.58, 153.39, 152.49, 145.23, 132.34, 131.44, 130.92 (d, $J = 11.3$ Hz), 125.06, 120.85 (d, $J = 11.3$ Hz), 120.30, 120.16, 119.22, 118.35 (d, $J = 94.3$ Hz), 114.31 (t, $J = 241.4$ Hz), 98.40, 98.00, 53.06 (t, $J = 25.9$ Hz), 18.64 (d, $J = 70.7$ Hz, 2C). IR (thin film, cm^{-1}) 3422.1, 2922.1, 2852.4, 1601.7, 1579.4, 1439.8, 1387.2, 1325.2, 1292.8, 755.6. HRMS calcd for $C_{19}H_{20}F_2N_7OP$, $[M+H]^+$, 432.1508; found 432.1509. $[M+Na]^+$, 454.1327; found 454.1322.

*5.1.7.15. (2-((2-((1-(2-Methoxyethyl)-1H-pyrazol-4-yl)amino)-7H-pyrrolo[2,3-d]pyrimidin-4-yl)amino)phenyl)dimethylphosphine oxide (**22c**).* White solid; yield: 82%; mp: 130.4–131.2 °C; ^{1}H NMR (600 MHz, DMSO-d_6) δ 11.53 (s, 1H), 11.17 (s, 1H), 9.08 (s, 1H), 8.77 (s, 1H), 7.93 (s, 1H), 7.60–7.54 (m, 2H), 7.52 (t, $J = 7.9$ Hz, 1H), 7.07 (t, $J = 7.3$ Hz, 1H), 6.89 (dd, $J = 3.3$, 2.3 Hz, 1H), 6.35 (dd, $J = 3.2$, 1.9 Hz, 1H), 4.19 (t, $J = 5.3$ Hz, 2H), 3.68 (t, $J = 5.3$ Hz, 2H), 3.24 (s, 3H), 1.83 (d, $J = 13.5$ Hz, 6H). ^{13}C NMR (150 MHz, DMSO-d_6) δ 155.70, 153.33, 152.61, 145.24, 132.29, 130.88 (d, $J = 11.3$ Hz), 130.16, 124.25, 120.77 (d, $J = 12.0$ Hz), 120.29, 119.73, 119.06, 118.29 (d, $J = 91.9$ Hz), 98.25, 97.94, 70.85, 58.04, 51.39, 18.63 (d, $J = 71.0$ Hz, 2C). Its ^{13}C NMR and DEPT spectrum displayed 20 carbon resonances for 3 primary carbon (δ_C 58.04, 18.63 × 2), 2 secondary carbon (δ_C 70.85, 51.39), 8 tertiary carbon (δ_C 132.29, 130.88, 130.16, 120.77, 120.29, 119.73, 119.06, 97.94), 7 quaternary carbon (δ_C 155.70, 153.33, 152.61, 145.24, 124.25, 118.29, 98.25). IR (thin film, cm^{-1}) 3424.6, 2922.2, 2852.3, 1828.3, 1439.8, 1384.8, 1291.5, 1118.2, 755.8. HRMS calcd for $C_{20}H_{24}N_7O_2P$, $[M+Na]^+$, 448.1621; found 448.1627.

*5.1.7.16. dimethyl(2-((2-((1-(tetrahydro-2H-pyran-4-yl)-1H-pyrazol-4-yl)amino)-7H-pyrrolo[2,3-d]pyrimidin-4-yl)amino)phenyl) phosphine oxide (**22d**).* Yellow solid; yield: 63%; mp: 196.4–197.0 °C; ^{1}H NMR (600 MHz, DMSO-d_6) δ 11.51 (s, 1H), 11.16 (s, 1H), 9.06 (s, 1H), 8.78 (s, 1H), 8.00 (s, 1H), 7.58 (dd, $J = 14.0$, 7.6 Hz, 1H), 7.54 (s, 1H), 7.50 (t, $J = 7.8$ Hz, 1H), 7.08 (t, $J = 7.3$ Hz, 1H), 6.89 (dd, $J = 3.2$, 2.3 Hz, 1H), 6.37–6.33 (m, 1H), 4.31 (ddd, $J = 15.5$, 11.1, 4.3 Hz, 1H), 3.97 (dd, $J = 11.1$, 3.2 Hz, 2H), 3.48 (td, $J = 11.6$, 1.9 Hz, 2H), 1.99–1.90 (m, 4H), 1.82 (d, $J = 13.5$ Hz, 6H). ^{13}C NMR (150 MHz, DMSO-d_6) δ 155.72, 153.38, 152.60, 145.23, 132.32, 130.94 (d, $J = 11.2$ Hz), 129.76, 124.17, 120.85 (d, $J = 10.1$ Hz), 120.39, 119.08, 118.48 (d, $J = 88.7$ Hz), 117.11, 98.24, 97.97, 66.01 (2C), 57.12, 33.12 (2C), 18.64 (d, $J = 70.7$ Hz, 2C). IR (thin film, cm^{-1}) 3425.1, 2922.9, 2851.9, 1601.3, 1578.7, 1440.8, 1385.8, 1325.0, 1292.3, 755.4. HRMS calcd for $C_{22}H_{26}N_7O_2P$, $[M+H]^+$, 452.1958; found 452.1960; $[M+Na]^+$, 474.1778; found 474.1778.

*5.1.7.17. Dimethyl(2-((2-((1-(piperidin-4-yl)-1H-pyrazol-4-yl) amino)-7H-pyrrolo[2,3-d]pyrimidin-4-yl)amino)phenyl)phosphine oxide hydrochloride (**22e**).* White solid; yield: 92%; mp: 247.3–248.2 °C; ^{1}H NMR (600 MHz, DMSO-d_6) δ 12.13 (s, 2H), 10.18 (s, 1H), 9.47 (s, 1H), 9.23 (s, 1H), 8.26 (s, 1H), 7.79 (s, 2H), 7.57 (s, 2H), 7.37 (s, 1H), 7.03 (s, 1H), 6.50 (s, 1H), 4.39 (s, 1H), 3.36 (d, $J = 10.1$ Hz, 2H), 3.07 (s, 2H), 2.16 (s, 4H), 1.79 (d, $J = 12.4$ Hz, 6H). ^{13}C NMR (150 MHz, DMSO-d_6) δ 155.77, 153.53, 152.74, 145.54, 132.26, 130.94 (d, $J = 11.0$ Hz), 129.43, 124.15, 120.60, 120.42, 119.07, 116.85, 98.42, 98.02, 59.18, 45.24 (2C), 33.77 (2C), 18.59 (d, $J = 70.6$ Hz, 2C). IR (thin film, cm^{-1}) 3426.6, 2922.5, 2852.3, 2343.6, 1638.9, 1546.1, 1463.5, 1384.0, 1124.8, 725.9. HRMS calcd for $C_{22}H_{27}N_8OP$, $[M+H]^+$, 451.2118; found 451.2123.

*5.1.7.18. 2-(4-((4-((2-(Dimethylphosphoryl)phenyl)amino)-7H-pyrrolo[2,3-d]pyrimidin-2-yl)amino)-1H-pyrazol-1-yl)-N,N-dimethylacetamide (**22f**).* White solid; yield: 62%; mp: 207.9–208.8 °C; ^{1}H NMR (600 MHz, DMSO-d_6) δ 11.55 (s, 1H), 11.17 (s, 1H), 9.08 (s, 1H), 8.83 (s, 1H), 7.89 (s, 1H), 7.54 (ddd, $J = 24.5$, 14.9, 7.8 Hz, 3H), 7.08 (s, 1H), 6.91–6.87 (m, 1H), 6.35 (d, $J = 0.9$ Hz, 1H), 5.03 (s, 2H), 3.04 (s, 3H), 2.87 (s, 3H), 1.83 (d, $J = 13.5$ Hz, 6H). ^{13}C NMR (150 MHz, DMSO-d_6) δ 166.94, 155.51, 153.36, 152.38, 145.18, 132.35, 130.87 (d, $J = 11.4$ Hz), 130.11, 124.43, 120.80 (d, $J = 9.4$ Hz), 120.47, 120.32, 119.09, 118.32 (d, $J = 98.3$ Hz), 98.26, 97.99, 53.06, 36.01, 35.21, 18.63 (d, $J = 70.9$ Hz, 2C). IR (thin film, cm^{-1}) 3424.0, 2922.6, 2852.3, 1639.6, 1579.7, 1475.3, 1438.7, 1385.0, 1123.1, 755.7. HRMS calcd for $C_{21}H_{25}N_8O_2P$, $[M+Na]^+$, 475.1730; found 475.1736.

*5.1.7.19. 2-(4-((4-((2-(Dimethylphosphoryl)phenyl)amino)-7H-pyrrolo[2,3-d]pyrimidin-2-yl)amino)-1H-pyrazol-1-yl)-1-morpholinoethan-1-one (**22g**).* Grey solid; yield: 65%; mp: 152.7–153.4 °C; ^{1}H NMR (600 MHz, DMSO-d_6) δ 11.53 (s, 1H), 11.16 (s, 1H), 9.07 (s, 1H), 8.81 (s, 1H), 7.90 (s, 1H), 7.59–7.49 (m, 3H), 7.06 (t, $J = 7.2$ Hz, 1H), 6.88 (dd, $J = 3.1$, 2.3 Hz, 1H), 6.34 (dd, $J = 3.0$, 1.9 Hz, 1H), 5.07 (s, 2H), 3.61–3.57 (m, 4H), 3.51 (d, $J = 6.5$ Hz, 2H), 3.46 (d, $J = 4.4$ Hz, 2H), 1.82 (d, $J = 13.5$ Hz, 6H). ^{13}C NMR (150 MHz, DMSO-d_6) δ 165.88, 155.61, 153.34, 152.61, 145.25, 132.35, 130.88 (d, $J = 11.4$ Hz), 130.17, 129.66, 124.61, 120.75 (d, $J = 11.5$ Hz), 120.37, 119.09, 98.28, 97.95, 66.06, 65.99, 52.93, 44.89, 41.81, 18.63 (d, $J = 70.5$ Hz, 2C). IR (thin film, cm^{-1}) 3364.3, 2920.8, 2850.5, 1657.7, 1633.2, 1580.0, 1468.9, 1403.2, 1240.2, 1116.4, 720.4. HRMS calcd for $C_{23}H_{27}N_8O_3P$, $[M+H]^+$, 495.2017; found 495.2022; $[M+Na]^+$, 517.1836; found 517.1847.

*5.1.7.20. 4-((4-((2-(Dimethylphosphoryl)phenyl)amino)-7H-pyrrolo [2,3-d]pyrimidin-2-yl)amino)-3-fluoro-N-(piperidin-4-yl)benzamide hydrochloride (**25a**).* White solid; yield: 87%; mp: 253.2–254.0 °C; ^{1}H NMR (600 MHz, DMSO-d_6) δ 12.16 (s, 2H), 9.73 (s, 1H), 9.11 (s, 2H), 8.62 (d, $J = 6.5$ Hz, 1H), 8.45 (s, 1H), 8.10 (s, 1H), 7.88 (d, $J = 11.7$ Hz, 1H), 7.76 (d, $J = 8.0$ Hz, 1H), 7.69 (dd, $J = 12.0$, 7.6 Hz, 1H), 7.45 (s, 1H), 7.25 (s, 1H), 7.09 (s, 1H), 6.49 (s, 1H), 3.31 (d, $J = 10.2$ Hz, 2H), 2.99 (s, 2H), 1.97 (d, $J = 11.7$ Hz, 2H), 1.89–1.80 (m, 8H). ^{13}C NMR (150 MHz, DMSO-d_6) δ 164.18, 153.71, 153.26 (d, $J = 245.5$ Hz), 151.23, 142.53, 132.46, 131.39 (d, $J = 10.5$ Hz), 130.03, 129.67, 129.59 (d, $J = 10.5$ Hz), 123.82, 123.62, 123.01, 122.49, 121.38, 114.64, 114.50, 99.69, 99.40, 44.58, 42.12 (2C), 28.11 (2C), 18.47 (d, $J = 70.8$ Hz, 2C). IR (thin film, cm^{-1}) 3424.8, 2924.2, 1639.2, 1618.8, 1541.5, 1501.6, 1463.3, 1383.0, 1339.0, 1311.0, 870.6, 736.0. HRMS calcd for $C_{26}H_{29}FN_7O_2P$, $[M+H]^+$, 522.2177; found 522.2180.

*5.1.7.21. 4-((4-((2-(Dimethylphosphoryl)phenyl)amino)-7H-pyrrolo [2,3-d]pyrimidin-2-yl)amino)-3-methoxy-N-(piperidin-4-yl)benzamide(**25b**).* White solid; yield: 83%; mp: 183.3–184.1 °C; ^{1}H NMR (600 MHz, DMSO-d_6) δ 11.64 (s, 1H), 11.57 (s, 1H), 8.90 (dd, $J = 8.1$, 3.8 Hz, 1H), 8.57 (d, $J = 8.6$ Hz, 1H), 8.17 (d, $J = 7.6$ Hz, 1H), 7.72 (s, 1H), 7.64–7.53 (m, 4H), 7.12 (t, $J = 7.2$ Hz, 1H), 7.04 (d, $J = 3.1$ Hz, 1H), 6.41 (d, $J = 3.1$ Hz, 1H), 3.98 (s, 3H), 3.86 (s, 1H), 2.98 (d, $J = 11.3$ Hz, 2H), 2.71–2.52 (m, 2H), 1.84 (d, $J = 13.5$ Hz, 6H), 1.75 (d, $J = 10.7$ Hz, 2H), 1.46 (dd, $J = 20.1$, 11.2 Hz, 2H). ^{13}C NMR (150 MHz, DMSO-d_6) δ 165.00, 154.60, 153.27, 151.74, 146.79, 144.75, 132.54, 132.48, 131.01 (d, $J = 11.1$ Hz), 126.62, 121.29 (d, $J = 12.0$ Hz), 120.56, 120.52, 120.21, 118.85 (d, $J = 91.8$ Hz), 116.56, 109.22, 99.67, 98.10, 56.07, 47.49, 45.52 (2C), 33.21 (2C), 18.58 (d, $J = 70.7$ Hz, 2C). Its ^{13}C NMR and DEPT spectrum displayed 27 carbon resonances for 3 primary carbon (δ_C 56.07, 18.58 × 2), 4 secondary carbon (δ_C 45.52 × 2, 33.21 × 2), 10 tertiary carbon (δ_C 132.48, 131.01, 121.29, 120.56, 120.52, 120.21, 116.56, 109.22, 98.10, 47.49), 10 quaternary carbon (δ_C 165.00, 154.60, 153.27, 151.74, 146.79, 144.75, 132.54, 126.62, 118.85, 99.67). IR (thin film, cm^{-1}) 3421.7, 2922.3, 2852.0, 1602.9, 1581.4, 1518.6, 1485.5, 1440.8, 1384.0, 1326.5, 1124.1, 755.8. HRMS calcd for $C_{27}H_{32}N_7O_3P$, $[M+Na]^+$, 556.2196; found 556.2192.

*5.1.7.22. 4-((4-((2-(Dimethylphosphoryl)phenyl)amino)-7H-pyrrolo [2,3-d]pyrimidin-2-yl)amino)-3-ethoxy-N-(piperidin-4-yl)benzamide (**25c**).* White solid; yield: 89%; mp: 246.1–246.8 °C; ^{1}H NMR

(600 MHz, DMSO-d_6) δ 11.63 (s, 1H), 11.52 (s, 1H), 8.90–8.84 (m, 1H), 8.58 (d, J = 8.2 Hz, 1H), 8.27 (d, J = 7.3 Hz, 1H), 7.69 (s, 1H), 7.62 (dd, J = 13.8, 7.6 Hz, 1H), 7.59–7.53 (m, 3H), 7.13 (t, J = 7.1 Hz, 1H), 7.05 (s, 1H), 6.40 (s, 1H), 4.24 (dd, J = 13.4, 6.6 Hz, 2H), 3.98–3.95 (m, 1H), 3.16 (d, J = 11.8 Hz, 2H), 2.77 (t, J = 11.8 Hz, 2H), 1.90–1.81 (m, 8H), 1.66 (dd, J = 21.6, 10.6 Hz, 2H), 1.47 (t, J = 6.7 Hz, 3H). ^{13}C NMR (150 MHz, DMSO-d_6) δ 165.26, 154.49, 153.26, 151.83, 145.83, 144.67, 132.80, 132.34, 131.04 (d, J = 11.2 Hz), 126.22, 121.40 (d, J = 12.0 Hz), 120.63, 120.58, 120.35, 119.09 (d, J = 91.8 Hz), 116.29, 110.22, 99.66, 98.12, 64.32, 45.99, 43.87 (2C), 30.74 (2C), 18.55 (d, J = 70.7 Hz, 2C), 14.70. IR (thin film, cm^{-1}) 3423.5, 2921.8, 2851.8, 1630.6, 1518.8, 1440.1, 1384.1, 1305.0, 1206.3, 1121.6, 865.7, 754.6. HRMS calcd for $C_{28}H_{34}N_7O_3P$, $[M+H]^+$, 548.2534; found 548.2544.

*5.1.7.23. 4-((4-((2-(Dimethylphosphoryl)phenyl)amino)-7H-pyrrolo [2,3-d]pyrimidin-2-yl)amino)-3-isopropoxy-N-(piperidin-4-yl)benzamide (**25d**).* Yellow solid; yield: 82%; mp: 172.4–174.6 °C; ^{1}H NMR (600 MHz, DMSO-d_6) δ 11.62 (s, 1H), 11.53 (s, 1H), 8.84 (dd, J = 8.2, 3.8 Hz, 1H), 8.57 (d, J = 8.4 Hz, 1H), 8.07 (d, J = 7.8 Hz, 1H), 7.65–7.59 (m, 2H), 7.56 (t, J = 7.8 Hz, 1H), 7.53 (s, 1H), 7.51 (d, J = 8.5 Hz, 1H), 7.12 (t, J = 7.2 Hz, 1H), 7.04 (d, J = 3.3 Hz, 1H), 6.38 (d, J = 3.3 Hz, 1H), 4.80–4.73 (m, 1H), 3.85–3.80 (m, 1H), 2.96 (d, J = 12.1 Hz, 2H), 1.83 (d, J = 13.5 Hz, 6H), 1.74 (d, J = 10.1 Hz, 2H), 1.46–1.36 (m, 8H). ^{13}C NMR (150 MHz, DMSO-d_6) δ 164.93, 154.42, 153.23, 151.86, 144.67, 144.49, 133.75, 132.26, 131.02 (d, J = 11.1 Hz), 126.43, 121.39 (d, J = 12.0 Hz), 120.66, 120.56 (d, J = 6.6 Hz), 120.41, 119.13 (d, J = 91.8 Hz), 116.35, 112.18, 99.62, 98.06, 71.37, 47.46, 45.49 (2C), 33.21 (2C), 21.96 (2C), 18.53 (d, J = 70.4 Hz, 2C). Its ^{13}C NMR and DEPT spectrum displayed 29 carbon resonances for 4 primary carbon (δ_C 21.96 × 2, 18.53 × 2), 4 secondary carbon (δ_C 45.49 × 2, 33.21 × 2), 11 tertiary carbon (δ_C 132.26, 131.02, 121.39, 120.66, 120.56, 120.41, 116.35, 112.18, 98.06, 71.37, 47.46), 10 quaternary carbon (δ_C 164.93, 154.42, 153.23, 151.86, 144.67, 144.49, 133.75, 126.43, 119.13, 99.62). IR (thin film, cm^{-1}) 3422.2, 2922.7, 2852.4, 1630.8, 1517.3, 1481.2, 1441.4, 1384.1, 1326.8, 1123.3, 755.8. HRMS calcd for $C_{29}H_{36}N_7O_3P$, $[M+H]^+$, 562.2690; found 562.2702.

*5.1.7.24. 4-((4-((2-(Dimethylphosphoryl)phenyl)amino)-7H-pyrrolo [2,3-d]pyrimidin-2-yl)amino)-N-(piperidin-4-yl)-3-(trifluoromethyl) benzamide (**25e**).* Grey solid; yield: 91%; mp: 183.8–184.6 °C; ^{1}H NMR (600 MHz, DMSO-d_6) δ 11.73 (s, 1H), 8.76 (d, J = 4.3 Hz, 1H), 8.46 (d, J = 7.7 Hz, 1H), 8.27 (d, J = 8.5 Hz, 1H), 8.22 (d, J = 1.5 Hz, 1H), 8.19–8.13 (m, 1H), 8.09–7.87 (m, 1H), 7.60–7.56 (m, 1H), 7.39 (t, J = 7.8 Hz, 1H), 7.07 (t, J = 7.3 Hz, 1H), 7.03 (d, J = 3.3 Hz, 1H), 6.39 (d, J = 3.4 Hz, 1H), 3.90–3.84 (m, 1H), 2.98 (d, J = 12.2 Hz, 2H), 2.51 (dd, J = 3.5, 1.7 Hz, 2H), 1.83 (d, J = 13.5 Hz, 6H), 1.77 (dd, J = 11.7, 2.1 Hz, 2H), 1.47–1.43 (m, 2H). ^{13}C NMR (150 MHz, DMSO-d_6) δ 163.72, 155.42, 153.16, 151.86, 144.80, 141.20, 132.20, 131.74, 130.92 (d, J = 11.3 Hz), 128.73, 124.17 (q, J = 273.4 Hz), 125.48 (d, J = 5.0 Hz), 125.16, 121.09 (d, J = 11.9 Hz), 120.62, 120.17 (d, J = 6.4 Hz), 119.64 (q, J = 29.0 Hz), 118.50 (d, J = 91.8 Hz), 99.86, 98.02, 47.69, 45.42 (2C), 33.09 (2C), 18.59 (d, J = 70.4 Hz, 2C). IR (thin film, cm^{-1}) 3447.5, 2922.3, 2852.3, 1637.1, 1546.0, 1512.5, 1442.5, 1384.1, 1304.5, 866.2, 754.4. HRMS calcd for $C_{27}H_{29}F_3N_7O_2P$, $[M+Na]^+$, 594.1965; found 594.1963.

*5.1.7.25. 4-((4-((2-(Dimethylphosphoryl)phenyl)amino)-7H-pyrrolo [2,3-d]pyrimidin-2-yl)amino)-2-fluoro-5-methoxy-N-(piperidin-4-yl) benzamide hydrochloride (**25f**).* White solid; yield: 86%; mp: 253.5–254.2 °C; ^{1}H NMR (600 MHz, DMSO-d_6) δ 12.45 (s, 1H), 12.02 (s, 1H), 9.16 (s, 3H), 8.35 (d, J = 7.3 Hz, 2H), 8.16 (d, J = 12.2 Hz, 1H), 7.76 (dd, J = 13.1, 7.7 Hz, 1H), 7.61 (t, J = 7.7 Hz, 1H), 7.34 (t, J = 7.2 Hz, 1H), 7.21 (d, J = 6.5 Hz, 1H), 7.14–7.11 (m, 1H), 6.54 (s, 1H), 4.07–4.02 (m, 1H), 3.91 (s, 3H), 3.28 (d, J = 12.5 Hz, 2H), 2.99 (dd, J = 21.1, 11.7 Hz, 2H), 1.99 (d, J = 10.7 Hz, 2H), 1.84–1.75 (m, 8H). ^{13}C NMR (150 MHz, DMSO-d_6) δ 163.05, 153.96, 153.42 (d, J = 240.7 Hz), 150.08, 144.42, 141.81, 132.70, 131.62 (d, J = 10.1 Hz), 130.64 (d, J = 12.3 Hz), 124.45, 123.52, 121.60, 116.54 (d, J = 11.5 Hz), 111.05, 111.03, 106.94 (d, J = 32.5 Hz), 100.06, 99.27, 56.57, 44.41, 41.90 (2C), 27.99 (2C), 18.39 (d, J = 70.7 Hz, 2C). IR (thin film, cm^{-1}) 3424.7, 2924.0, 2852.4, 1616.9, 1537.4, 1498.1, 1463.0, 1387.0, 1300.3, 1121.7, 873.3, 756.1. HRMS calcd for $C_{27}H_{31}FN_7O_3P$, $[M+H]^+$, 552.2283; found 552.2287.

*5.1.7.26. 4-((4-((2-(Dimethylphosphoryl)phenyl)amino)-7H-pyrrolo [2,3-d]pyrimidin-2-yl)amino)-2-methyl-N-(piperidin-4-yl)benzamide (**25g**).* White solid; yield: 81%; mp: 243.7–244.2 °C; ^{1}H NMR (400 MHz, DMSO-d_6) δ 11.66 (s, 1H), 11.37 (s, 1H), 9.11 (dd, J = 8.1, 3.9 Hz, 1H), 9.07 (s, 1H), 7.93 (d, J = 7.9 Hz, 1H), 7.69 (d, J = 7.4 Hz, 2H), 7.61–7.50 (m, 2H), 7.23 (d, J = 8.2 Hz, 1H), 7.08 (t, J = 7.1 Hz, 1H), 6.97 (d, J = 2.8 Hz, 1H), 6.39 (d, J = 2.9 Hz, 1H), 3.81–3.71 (m, 1H), 2.94 (d, J = 11.9 Hz, 2H), 2.35 (s, 3H), 1.84 (d, J = 13.5 Hz, 6H), 1.74 (d, J = 11.6 Hz, 2H), 1.42–1.32 (m, 2H). ^{13}C NMR (150 MHz, DMSO-d_6) δ 168.16, 155.19, 153.08, 151.89, 145.10, 142.46, 135.79, 132.45, 130.90 (d, J = 11.2 Hz), 129.03, 127.79, 120.87 (d, J = 11.9 Hz), 120.23 (d, J = 6.3 Hz), 120.03, 119.44, 118.18 (d, J = 91.9 Hz), 114.70, 99.28, 97.99, 47.05, 45.30, 33.09 (2C), 20.18 (2C), 18.66 (d, J = 70.8 Hz, 2C). IR (thin film, cm^{-1}) 3423.5, 2921.6, 2851.5, 1630.4, 1543.2, 1439.4, 1384.4, 1304.4, 1241.5, 867.9, 754.5. HRMS calcd for $C_{27}H_{32}N_7O_2P$, $[M+H]^+$, 518.2428; found 518.2432; $[M+Na]^+$, 540.2247; found 540.2257.

*5.1.7.27. 4-((4-((2-(Dimethylphosphoryl)phenyl)amino)-7H-pyrrolo [2,3-d]pyrimidin-2-yl)amino)-2-fluoro-N-(piperidin-4-yl)benzamide (**25h**).* White solid; yield: 88%; mp: 277.4–278.5 °C; ^{1}H NMR (400 MHz, DMSO-d_6) δ 11.70 (s, 1H), 11.56 (s, 1H), 9.51 (s, 1H), 9.07 (dd, J = 8.2, 4.0 Hz, 1H), 8.08 (d, J = 14.2 Hz, 1H), 7.76 (dd, J = 7.5, 3.3 Hz, 1H), 7.62–7.51 (m, 4H), 7.11 (t, J = 7.2 Hz, 1H), 7.04 (d, J = 3.3 Hz, 1H), 6.42 (d, J = 3.3 Hz, 1H), 3.86–3.77 (m, 1H), 2.94 (d, J = 12.2 Hz, 2H), 2.53–2.48 (m, 2H), 1.84 (d, J = 13.5 Hz, 6H), 1.76 (d, J = 10.6 Hz, 2H), 1.44–1.34 (m, 2H). ^{13}C NMR (100 MHz, DMSO-d_6) δ 162.75, 160.01 (d, J = 244.9 Hz), 154.58, 153.14, 151.50, 145.37 (d, J = 12.4 Hz), 144.90, 132.44, 130.92 (d, J = 11.3 Hz), 130.19 (d, J = 4.6 Hz), 121.11 (d, J = 12.0 Hz), 120.51, 120.41 (d, J = 7.0 Hz), 118.53 (d, J = 91.8 Hz), 114.58 (d, J = 14.1 Hz), 113.21, 103.98 (d, J = 29.1 Hz), 99.68, 98.05, 47.27, 45.18 (2C), 32.98 (2C), 18.61 (d, J = 70.7 Hz, 2C). IR (thin film, cm^{-1}) 3413.8, 2921.5, 2851.7, 1627.3, 1523.3, 1384.4, 1242.2, 866.6, 754.4. HRMS calcd for $C_{26}H_{29}FN_7O_2P$, $[M+H]^+$, 522.2177; found 552.2183.

*5.1.8. General procedure for the synthesis of intermediates **28a-f***

4-nitro-1*H*-pyrazole (1 equiv), corresponding alcohols (1 equiv) and triphenylphosphine (1.5 equiv) were dissolved in THF, and di-tert-butyl azodicarboxylate (1.5 equiv) was added over approximately 10 min. The resulting mixture was stirred at room temperature for 5 h and concentrated to dryness. The residue was purified by column chromatography to give intermediates **27a-c**. A solution of 4-nitro-1*H*-pyrazole (1 equiv), potassium carbonate (1 equiv) and the alkylating reagent (1.1 eq) in acetonitrile was heated at 40–80 °C for 8 h. The mixture was diluted with ethyl acetate, and the organic layer was washed with brine, dried over anhydrous Na_2SO_4 and filtered. The filtrate was concentrated and purified by chromatography to give intermediates **27b-f**. Intermediates **27a-f** (1 equiv) were dissolved in ethanol, and Pd/C (0.1 equiv) was added. The flask was flushed with H_2 and stirred for 3 h at 40 °C. The reaction mixture was filtered through a Celite pad and the filtrate was concentrated to dryness, yielding intermediates **28a-f**.

*5.1.9. General procedure for the synthesis of compounds **31a-h***

To a solution of tert-butyl 4-aminopiperidine-1-carboxylate (1

equiv) and appropriate acids (1 equiv) in CH_2Cl_2 at rt, HATU (1.2 equiv) and DIEA (1.5 equiv) were added. The resulting mixture was warmed to 25 °C-40 °C and stirred until completion of the reaction. The mixture was diluted with ethyl acetate, and the organic layer was washed with brine, dried over anhydrous Na_2SO_4 and filtered. The filtrate was concentrated and purified by chromatography to yield the intermediates **30a-h**. Intermediates **30a-h** (1 equiv) were dissolved in ethanol, and Pd/C (0.1 equiv) was added. The flask was flushed with H_2 and stirred for 3 h at 40 °C. The reaction mixture was filtered through a Celite pad and the filtrate was concentrated to dryness, yielding intermediates **31a-h**.

*5.1.10. Preparation of compounds **34b**, **35**, **38b** and **39***

Compounds **34b**, **35**, **38b** and **39** were prepared in a similar manner as compounds **11a-h**.

*5.1.10.1. (2-((2-((1-(2-Methoxyethyl)-1H-pyrazol-4-yl)amino)-7H-pyrrolo[2,3-d]pyrimidin-4-yl)amino)phenyl)dimethylphosphine oxide (**34b**).* White solid; yield: 47%; mp: 128.7–129.2 °C; ^{1}H NMR (400 MHz, $CDCl_3$) δ 11.48 (s, 1H), 8.92 (s, 1H), 7.96 (s, 1H), 7.58–7.42 (m, 3H), 7.25–7.17 (m, 1H), 7.05 (s, 1H), 7.00–6.89 (m, 2H), 4.26 (s, 2H), 3.77 (s, 2H), 3.33 (s, 3H), 1.84 (d, J = 13.0 Hz, 6H). ^{13}C NMR (100 MHz, $CDCl_3$) δ 169.14, 156.88, 155.07, 145.08 (d, J = 2.7 Hz), 132.99, 132.99 (d, J = 1.9 Hz), 129.78 (d, J = 11.2 Hz), 123.08, 121.93, 121.8, 121.77, 118.69, 118.20 (d, J = 98.6 Hz), 118.18, 112.52, 71.43, 59.10, 52.47, 19.04 (d, J = 71.7 Hz, 2C). IR (thin film, cm^{-1}) 3438.0, 2922.3, 2852.2, 1628.1, 1384.2, 1106.1, 580.1. HRMS calcd for $C_{20}H_{23}N_6O_2PS$, $[M+Na]^+$, 465.1233; found 465.1238.

*5.1.10.2. 4-((4-((2-(Dimethylphosphoryl)phenyl)amino)thieno[2,3-d]pyrimidin-2-yl)amino)-3-methoxy-N-(piperidin-4-yl)benzamide hydrochloride (**35**).* Yellow solid; yield: 89%; mp: 223.7–224.4 °C; ^{1}H NMR (600 MHz, DMSO-d_6) δ 12.44 (s, 1H), 9.20–9.03 (m, 3H), 8.72 (s, 1H), 8.57 (d, J = 7.3 Hz, 1H), 8.02 (d, J = 8.0 Hz, 1H), 7.69 (dd, J = 13.1, 7.6 Hz, 1H), 7.63 (d, J = 1.5 Hz, 1H), 7.57 (dd, J = 8.3, 1.6 Hz, 1H), 7.50 (dd, J = 17.1, 6.9 Hz, 2H), 7.45 (d, J = 5.9 Hz, 1H), 7.23 (t, J = 7.3 Hz, 1H), 4.11–4.06 (m, 1H), 3.93 (s, 3H), 3.31 (d, J = 12.4 Hz, 2H), 3.00 (dd, J = 22.1, 12.0 Hz, 2H), 2.01–1.96 (m, 2H), 1.89–1.83 (m, 8H). ^{13}C NMR (150 MHz, DMSO-d_6) δ 172.01, 165.30, 154.55, 154.40, 149.89, 143.14, 132.51, 131.25 (d, J = 11.2 Hz), 130.01, 123.14 (d, J = 11.7 Hz), 121.56 (d, J = 6.2 Hz), 121.46, 120.80, 120.38 (d, J = 90.6 Hz), 120.16, 118.58, 112.91, 110.30, 56.10, 44.64, 42.19 (2C), 28.23 (2C), 18.51 (d, J = 70.8 Hz, 2C). IR (thin film, cm^{-1}) 3450.9, 2923.3, 2852.6, 1627.0, 1546.9, 1526.1, 1441.6, 1384.4, 1340.0, 1109.2, 873.5, 754.5. HRMS calcd for $C_{27}H_{31}N_6O_3PS$, $[M+H]^+$, 551.1989; found 551.1995.

*5.1.10.3. (2-((2-((1-(2-Methoxyethyl)-1H-pyrazol-4-yl)amino)thieno[3,2-d]pyrimidin-4-yl)amino)phenyl)dimethylphosphine oxide (**38b**).* White solid; yield: 38%; mp: 96.5–97.6 °C; ^{1}H NMR (400 MHz, $CDCl_3$) δ 11.30 (s, 1H), 8.82 (dd, J = 8.1, 4.2 Hz, 1H), 7.94 (s, 1H), 7.67 (d, J = 5.2 Hz, 1H), 7.53 (dd, J = 16.2, 8.3 Hz, 2H), 7.29–7.19 (m, 2H), 7.08 (t, J = 6.7 Hz, 1H), 7.01 (s, 1H), 4.26 (t, J = 5.3 Hz, 2H), 3.77 (t, J = 5.3 Hz, 2H), 3.33 (s, 3H), 1.85 (d, J = 13.2 Hz, 6H). ^{13}C NMR (100 MHz, $CDCl_3$) δ 161.70, 158.10, 155.34, 144.91 (d, J = 2.5 Hz), 132.91 (d, J = 2.0 Hz), 132.58, 131.93, 129.78 (d, J = 11.2 Hz), 123.86, 123.32, 122.37 (d, J = 7.2 Hz), 122.17 (d, J = 12.4 Hz), 121.83, 118.60 (d, J = 95.1 Hz), 109.87, 71.46, 59.12, 52.48, 19.03 (d, J = 71.4 Hz, 2C). IR (thin film, cm^{-1}) 3441.2, 2923.0, 2852.6, 1633.2, 1384.1, 1116.9, 867.2, 469.8. HRMS calcd for $C_{20}H_{23}N_6O_2PS$, $[M+H]^+$, 443.1414; found 443.1420.

*5.1.10.4. 4-((4-((2-(Dimethylphosphoryl)phenyl)amino)thieno[3,2-d]pyrimidin-2-yl)amino)-3-methoxy-N-(piperidin-4-yl)benzamide (**39**).* White solid; yield: 83%; mp: 193.5–194.2 °C; ^{1}H NMR (400 MHz, DMSO-d_6) δ 8.72 (dd, J = 7.5, 3.5 Hz, 1H), 8.46 (d, J = 8.8 Hz, 1H), 8.11 (t, J = 6.3 Hz, 2H), 7.93 (s, 1H), 7.65 (dd, J = 13.8, 7.7 Hz, 1H), 7.60–7.50 (m, 3H), 7.29 (d, J = 5.3 Hz, 1H), 7.19 (t, J = 7.2 Hz, 1H), 3.96 (s, 3H), 3.90–3.81 (m, 1H), 2.98 (d, J = 11.4 Hz, 2H), 2.55 (s, 2H), 1.83 (d, J = 13.6 Hz, 6H), 1.76 (d, J = 11.5 Hz, 2H), 1.49–1.39 (m, 2H). ^{13}C NMR (150 MHz, DMSO-d_6) δ 164.96, 161.34, 157.18, 154.78, 147.53, 144.11, 134.14, 132.34, 132.05, 131.08 (d, J = 10.8 Hz), 127.55, 123.80, 122.25, 121.92 (d, J = 6.5 Hz), 120.39 (d, J = 94.5 Hz), 120.08, 117.93, 109.94, 109.35, 56.01, 47.45, 45.46 (2C), 33.16 (2C), 18.42 (d, J = 70.6 Hz, 2C). IR (thin film, cm^{-1}) 3426.5, 2922.3, 2852.1, 1636.1, 1547.0, 1510.8, 1438.5, 1384.3, 1109.2, 868.0, 755.8. HRMS calcd for $C_{27}H_{31}N_6O_3PS$, $[M+H]^+$, 551.1989; found 551.1985.

5.2. Pharmacological assay

5.2.1. FAK HTRF assay

The FAK kinase assay was performed using the HTRF® KinEASE™-TK kit (Cisbio Bioassays, France) in white 384-well small volume plates with a total working volume of 20 μL. Purified FAK enzyme was purchased from Carna Biosciences (Japan). Compounds were diluted step-by-step from a concentrated stock of 8 mM in 100% DMSO and with serial kinase reaction buffer dilutions. The IC_{50} measurements were performed in replicates. For each assay, 4 μL of dispensed compounds, 4 μL of mix 1 (ATP + Substrate TK) and 2 μL of kinase (0.111 ng/μL) were added to the assay wells. The assay plates were incubated at 30 °C for 50 min and reactions were terminated by adding 10 μL of mix 2 (Sa-XL665+TK-Antibody-Cryptate). After a final incubation (60 min at room temperature), HTRF signals were obtained by reading plates using an Infinite® F500 microplate reader (Tecan, Switzerland). The fluorescence was measured at 620 nM (Cryptate) and 665 nM (XL665). A ratio was calculated (665/620) for each well. For IC_{50} measurements, values were normalized and fitted with Prism (GraphPad software).

5.2.2. Cell proliferation assay

The antiproliferative activities of the new synthesized compounds were evaluated against A549, MDA-MB-231 and HK2 cell lines by the standard MTT assay *in vitro* [30]. TAE-226 was employed as the positive control. The cell lines were suspended in medium to adjust their concentration to approximate 5×10^4 cells/mL. The suspension was dispensed at 100 μL/well to a 96-well plate and at 37 °C in a humidified atmosphere with 5% CO_2 for 24 h. The tested compounds at the indicated final concentrations were added to the culture medium and incubated for 72 h. Fresh MTT was added to each well at the terminal concentration of 5 mg/mL in PBS, and incubated with cells at 37 °C for 4 h. The formazan crystals in each well were dissolved in 150 mL DMSO, and the absorbency of each test well was performed at λ_{490nm} by a Thermo reader (Mulitiskan go).

5.2.3. Analysis of cell apoptosis

The ability of **25b** to induce apoptosis of A549 cells was quantified by annexin V and PI staining and flow cytometry. The Annexin V-FITC Apoptosis Kit was purchased from US Everbright® Inc. Briefly, after treatment with **25b** for 72 h, cells were harvested, washed with PBS twice, and subjected to annexin V and propidium iodide staining using the annexin V FITC apoptosis kit following the step-by-step protocol provided by the manufacturer. After staining, flow cytometry was performed for the quantification of apoptotic cells.

5.2.4. Cell migration assay

A transwell chamber assay was conducted in Transwell

chambers (Corning Incorporated). The cells were trypsinized and reseeded in the upper chamber at a concentration of 1×10^5/mL in 100 μL. The lower chambers were filled with 500 μL DMEM containing 10% serum. After incubation with compound **25b**, the cells that had not migrated from the top surface of the filters were removed with cotton and the cells on the lower surface were fixed in 100% methanol and stained with 0.25% crystal violet. Migrated cells were quantitated by counting cells in six randomly selected fields on each filter under a microscope at 200x magnification and photographed [31].

5.2.5. Liver microsomal stability assay

The liver microsomal stability assay was performed by incubating with microsomes (human microsome, Corning, lot No. 38292; rat microsome, Xenotech, Lot No. 1310030; and mouse microsome, Xenotech, Lot No. 1710069) (0.5 mg/mL) at 37 °C with compound **25 b** at a final concentration of 1 μM in potassium phosphate buffer (pH 7.4, 100 mM with 10 mM $MgCl_2$). The incubation was initiated by the addition of prewarmed cofactors (1 mmol NADPH). After incubation at 37 °C for different times (0, 5, 10, 20, 30, and 60 min), the protein was precipitated by the addition of cold acetonitrile. Then, the precipitated proteins were then removed by centrifugation, and the supernatants were injected into an LC-MS/MS system. The metabolic stability tests of mice, rats and human livers are fully in accordance with the Guide for the Care and Use of Laboratory Animals.

5.2.6. Cytochrome P450 inhibition assay

Cytochrome P450 inhibition was tested in human liver microsomes (0.253 mg/mL) using five probe substrates (CYP3A4, midazolam; CYP2C19, S-mephenytoin; CYP2C9, diclofenac; CYP1A2, phenacetin; and CYP2D6, dextromethorphan) in the presence of compound **25b** (10 μM). After preincubation for 10 min at 37 °C, an NADPH-regenerating system was added. After the mixed system was incubated for 15 min at 37 °C, the reaction was stopped by adding 400 μL of cold stop solution (200 ng/mL labetalol and 200 ng/mL tolbutamide in acetonitrile). The incubation mixtures were then centrifuged, and the supernatants were analyzed by LC/MS/MS.

5.2.7. Molecular docking study

Ligand structures were prepared by using Maestro 9.0 within the Schrödinger package. The crystal structures of FAK (PDB ID: 2JKK) were retrieved from RCSB Protein Data Bank (http://www.pdb.org), and prepared for molecular docking by using Protein Preparation Wizard. The ligand structures were optimized by Maestro's Ligprep module, regulated to a protonated state of pH 7.4, and minimized with OPLS 2005 force field to produce low-energy conformers. Compounds were docked into binding sites with the Glide module within the Schrödinger package on account of united-atom scoring function. The docking program was implemented twenty times, providing sufficient constellation groups and the output was characterized by the favorable binding affinity value. In addition, the figure was prepared using PyMOL.

Acknowledgments

We gratefully acknowledge the financial support from the Program for Innovative Research Team of the Ministry of Education and Program for Liaoning Innovative Research Team in University.

Appendix A. Supplementary data

Supplementary data to this article can be found online at https://doi.org/10.1016/j.ejmech.2019.111716.

References

[1] M.D. Schaller, Cellular functions of FAK kinases: insight into molecular mechanisms and novel functions, J. Cell Sci. 123 (2010) 1007–1013.
[2] M.C. Frame, P. Hitesh, S. Bryan, L. Daniel, M.J. Eck, The FERM domain: organizing the structure and function of FAK, Nat. Rev. Mol. Cell Biol. 11 (2010) 802–814.
[3] C. Bã©Raud, V. Dormoy, S. Danilin, V. Lindner, A. Bã©Thry, M. Hochane, C. Coquard, M. Barthelmebs, D. Jacqmin, H. Lang, Targeting FAK scaffold functions inhibits human renal cell carcinoma growth, Int. J. Cancer 137 (2015) 1549–1559.
[4] P. Yuliya, K.M. Gillen, G. William, H.E. Beggs, L.F. Reichardt, F.G. Giancotti, Ras- and PI3K-dependent breast tumorigenesis in mice and humans requires focal adhesion kinase signaling, J. Clin. Investig. 119 (2009) 252–266.
[5] L. Tanguy, H.D. Kairbaan, Focal adhesion kinase and tumour angiogenesis, J. Pathol. 226 (2012) 404–412.
[6] S. Joerg, D. Neesha, D.W. Hedley, Targeting focal adhesion kinase signaling in tumor growth and metastasis, Expert Opin. Ther. Targets 14 (2010) 77–94.
[7] J. Zhao, J.L. Guan, Signal transduction by focal adhesion kinase in cancer, Cancer Metastasis Rev. 28 (2009) 35–49.
[8] B.Y. Lee, P. Timpson, L.G. Horvath, R.J. Daly, FAK signaling in human cancer as a target for therapeutics, Pharmacol. Ther. 146 (2015) 132–149.
[9] Z. Liu, Y. Zhou, W. Wu, Effect of antisense oligonucleotides targeting focal adhesion kinase on the proliferation and activation of hepatic stellate cells, J. Biomed. Eng. 25 (2008) 419–423.
[10] K. Tsutsumi, T. Kasaoka, H.M. Park, H. Nishiyama, M. Nakajima, T. Honda, Tumor growth inhibition by synthetic and expressed siRNA targeting focal adhesion kinase, Int. J. Oncol. 33 (2008) 215–224.
[11] H. Jiang, S. Hegde, B.L. Knolhoff, Y. Zhu, J.M. Herndon, M.A. Meyer, T.M. Nywening, W.G. Hawkins, I.M. Shapiro, D.T. Weaver, Targeting focal adhesion kinase renders pancreatic cancers responsive to checkpoint immunotherapy, Nat. Med. 22 (2016) 851–860.
[12] S. Alan, L. Tom, S. Bryan, B. Adam, R.C. Mcpherson, V.K. Alexander, G.C. Laura, C. Marta, M. Morwenna, J.E. Ring, Nuclear FAK controls chemokine transcription, tregs, and evasion of anti-tumor immunity, Cell 163 (2015) 160–173.
[13] K.J. Tang, J. Constanzo, N. Venkateswaran, M. Melegari, M. Ilcheva, J.C. Morales, F. Skoulidis, J.V. Heymach, D.A. Boothman, P.P. Scaglioni, Focal Adhesion Kinase regulates the DNA damage response and its inhibition radiosensitizes mutant KRAS lung cancer, Clin. Cancer Res. Off. J. Am. Assoc. Cancer Res. 22 (2016) 5851–5863.
[14] N. Kurio, T. Shimo, T. Fukazawa, T. Okui, N.M. Hassan, T. Honami, Y. Horikiri, S. Hatakeyama, M. Takaoka, Y. Naomoto, Anti-tumor effect of a novel FAK inhibitor TAE226 against human oral squamous cell carcinoma, Oral Oncol. 48 (2012) 1159–1170.
[15] R.T. Kurmasheva, R. Gorlick, E.A. Kolb, S.T. Keir, J.M. Maris, R.B. Lock, H. Carol, M. Kang, C.P. Reynolds, J. Wu, Initial testing of VS-4718, a novel inhibitor of focal adhesion kinase (FAK), against pediatric tumor models by the Pediatric Preclinical Testing Program, Pediatr. Blood Cancer (2016) 64.
[16] G.R. Ott, M. Cheng, K.S. Learn, J. Wagner, D.E. Gingrich, J.G. Lisko, M. Curry, E.F. Mesaros, A.K. Ghose, M.R. Quail, Discovery of clinical candidate CEP-37440, a selective inhibitor of focal adhesion kinase (FAK) and anaplastic lymphoma kinase (ALK), J. Med. Chem. 59 (2016) 7478–7496.
[17] Y. Kang, W. Hu, C. Ivan, H.J. Dalton, T. Miyake, C.V. Pecot, B. Zand, T. Liu, J. Huang, N.B. Jennings, Role of focal adhesion kinase in regulating YB-1-mediated paclitaxel resistance in ovarian cancer, J. Natl. Cancer Inst. 105 (2013) 1485–1495.
[18] J.R. Infante, D.R. Camidge, L.R. Mileshkin, E.X. Chen, R.J. Hicks, D. Rischin, H. Fingert, K.J. Pierce, H. Xu, W.G. Roberts, Safety, pharmacokinetic, and pharmacodynamic phase I dose-escalation trial of PF-00562271, an inhibitor of focal adhesion kinase, in advanced solid tumors, J. Clin. Oncol. Off. J. Am. Soc. Clin. Oncol. 30 (2012) 1527–1533.
[19] N.F. Brown, M. Williams, H.T. Arkenau, R.A. Fleming, J. Tolson, L. Yan, J. Zhang, L. Swartz, R. Singh, K.R. Auger, A study of the focal adhesion kinase inhibitor GSK2256098 in patients with recurrent glioblastoma with evaluation of tumor penetration of [11C]GSK2256098, Neuro Oncol. 20 (2018) 1634–1642.
[20] M. Qu, Z. Liu, D. Zhao, C. Wang, J. Zhang, Z. Tang, K. Liu, X. Shu, H. Yuan, X. Ma, Design, synthesis and biological evaluation of sulfonamide-substituted diphenylpyrimidine derivatives (Sul-DPPYs) as potent focal adhesion kinase (FAK) inhibitors with antitumor activity, Biorg. Med. Chem. 25 (2017) 3989–3996.
[21] L. Wang, M. Ai, J. Yu, L. Jin, C. Wang, Z. Liu, X. Shu, Z. Tang, K. Liu, H. Luo, Structure-based modification of carbonyl-diphenylpyrimidines (Car-DPPYs) as a novel focal adhesion kinase (FAK) inhibitor against various stubborn cancer cells, Eur. J. Med. Chem. 172 (2019) 154–162.
[22] Y. Su, R. Li, X. Ning, Z. Lin, X. Zhao, J. Zhou, J. Liu, Y. Jin, Y. Yin, Discovery of 2,4-diarylaminopyrimidine derivatives bearing dithiocarbamate moiety as novel FAK inhibitors with antitumor and anti-angiogenesis activities, Eur. J. Med. Chem. 177 (2019) 32–46.
[23] C.R. Coxon, E. Anscombe, S.J. Harnor, M.P. Martin, B. Carbain, B.T. Golding, I.R. Hardcastle, L.K. Harlow, S. Korolchuk, C.J. Matheson, Cyclin-dependent kinase (CDK) inhibitors: structure–activity relationships and insights into the CDK-2 selectivity of 6-substituted 2-arylaminopurines, J. Med. Chem. 60 (2017) 1746–1767.

[24] W. Kawahata, T. Asami, T. Irie, M. Sawa, Design and synthesis of novel pyrimidine analogs as highly selective, non-covalent BTK inhibitors, Bioorg. Med. Chem. Lett 28 (2017) 145–151.
[25] B.A. Lefker, J. Shin, C.M.M. Williams, K.F. Geoghegan, S.W. Wright, D.C. Limburg, P.D. Bonin, S.J. Ramsey, W. Jiang, P. Sahasrabudhe, Correction: design and chemoproteomic functional characterization of a chemical probe targeted to bromodomains of BET family proteins, Med.chem.commun 6 (2015), 247-247.
[26] W.-S. Huang, S. Liu, D. Zou, R.M. Thomas, Y. Wang, T. Zhou, J. Romero, A. Kohlmann, F. Li, J. Qi, Discovery of brigatinib (AP26113), a phosphine oxide-containing, potent, orally active inhibitor of anaplastic lymphoma kinase, J. Med. Chem. 59 (2016) 4948–4964.
[27] G.R. Ott, G.J. Wells, T.V. Thieu, M.R. Quail, J.G. Lisko, E.F. Mesaros, D.E. Gingrich, A.K. Ghose, W. Weihua, L. Lihui, 2,7-disubstituted-pyrrolo[2,1-f][1,2,4]triazines: new variant of an old template and application to the discovery of anaplastic lymphoma kinase (ALK) inhibitors with in vivo antitumor activity, J. Med. Chem. 54 (2011) 6328–6341.
[28] L. Yao, K. Li, W. Peng, Q. Lin, S. Li, X. Hu, X. Zheng, Z. Shao, An aberrant spliced transcript of focal adhesion kinase is exclusively expressed in human breast cancer, J. Transl. Med. 12 (2014) 136.
[29] B. Zhou, G.Z. Wang, Z.S. Wen, Y.C. Zhou, Y.C. Huang, Y. Chen, G.B. Zhou, Somatic mutations and splicing variants of focal adhesion kinase in non-small cell lung cancer, J. Natl. Cancer Inst. 110 (2018) 195–204.
[30] L. He, B. Wu, G. Yang, J. Xu, S. Song, C. Wang, J. Yao, K. Liu, Y. Li, X. Sun, Phosphamide-containing diphenylpyrimidine analogues (PA-DPPYs) as potent focal adhesion kinase (FAK) inhibitors with enhanced activity against pancreatic cancer cell lines, Biorg. Med. Chem. 25 (2017) 6313–6321.
[31] J. Guo, M. Zhu, T. Wu, C. Hao, K. Wang, Z. Yan, W. Huang, J. Wang, D. Zhao, M. Cheng, Discovery of indolin-2-one derivatives as potent PAK4 inhibitors: structure-activity relationship analysis, biological evaluation and molecular docking study, Biorg. Med. Chem. 25 (2017) 3500–3511.